CENTRAL RESEARCH LIBRARY
DOCUMENT COLLECTION

MARTIN MARIETTA ENERGY SYSTEMS LIBRARIES
3 4456 0250710 6

ORNL-2292
Volume 1
Physics and Mathematics

A MONTE CARLO CALCULATION OF AIR-SCATTERED GAMMA RAYS

R. E. Lynch
J. W. Benoit
W. P. Johnson
C. D. Zerby

CENTRAL RESEARCH LIBRARY
DOCUMENT COLLECTION
LIBRARY LOAN COPY
DO NOT TRANSFER TO ANOTHER PERSON
If you wish someone else to see this document, send in name with document and the library will arrange a loan.

OAK RIDGE NATIONAL LABORATORY
operated by
UNION CARBIDE CORPORATION
for the
U.S. ATOMIC ENERGY COMMISSION

Printed in USA. Price 2.00 cents. Available from the

Office of Technical Services
U. S. Department of Commerce
Washington 25, D. C.

LEGAL NOTICE

This report was prepared as an account of Government sponsored work. Neither the United States, nor the Commission, nor any person acting on behalf of the Commission:

A. Makes any warranty or representation, express or implied, with respect to the accuracy, completeness, or usefulness of the information contained in this report, or that the use of any information, apparatus, method, or process disclosed in this report may not infringe privately owned rights; or

B. Assumes any liabilities with respect to the use of, or for damages resulting from the use of any information, apparatus, method, or process disclosed in this report.

As used in the above, "person acting on behalf of the Commission" includes any employee or contractor of the Commission to the extent that such employee or contractor prepares, handles or distributes, or provides access to, any information pursuant to his employment or contract with the Commission.

UNCLASSIFIED

ORNL-2292
Volume 1

Copy No. _____

Contract No. W-7405-eng-26

NEUTRON PHYSICS DIVISION*

A MONTE CARLO CALCULATION OF AIR-SCATTERED GAMMA RAYS

R. E. Lynch** W. P. Johnson**
J. W. Benoit** C. D. Zerby

Date Issued

OAK RIDGE NATIONAL LABORATORY
Oak Ridge, Tennessee
operated by
UNION CARBIDE CORPORATION
for the
U. S. ATOMIC ENERGY COMMISSION

MARTIN MARIETTA ENERGY SYSTEMS LIBRARIES
3 4456 0250710 6

UNCLASSIFIED

*Previously known as the Applied Nuclear Physics Division.
**Wright Air Development Center.

ABSTRACT

A calculation is presented of air-scattered gamma rays using the Monte Carlo method of computation. For simplicity, the problem was idealized to have a monoenergetic, monodirectional point source of gamma rays in an infinite body of air. The results of the calculation included the angular distributions, energy spectra, and tissue dose rates at source-detector separation distances of from 5 to 100 ft. A complete parameter survey was completed for source energies from 0.6 to 12 Mev and for beam angles with respect to the source-detector axis of from 0 to 180 deg. The report is divided into five volumes: Volume 1 gives a complete description of the mathematical procedure used in the calculation, while volumes 2 and 3 present tables of data representing the energy spectra and angular distributions obtained from the calculation. Volumes 4 and 5 present information similar to that in volumes 2 and 3, except that the data have been converted to tissue dose rates.

PREFACE

This calculation was performed by the Power Plant Laboratory at Wright Air Development Center. The problem was initiated at Oak Ridge National Laboratory (ORNL) during the one-month visit of Lt. R. E. Lynch of WADC. It was suggested by and designed from a theoretical point of view by C. D. Zerby of ORNL who also acted as advisor throughout the duration of the computation. The calculation was set up and coded for the Remington Rand 1103 computer, located at WADC, by Lt. Lynch, who obtained aid with the coding of a portion of the problem from Lt. L. W. Benoit. Lieutenants Lynch, Benoit, and W. P. Johnson, all of WADC, carried out the analysis of the completed calculation.

TABLE OF CONTENTS

		Page No.
	Abstract	iii
	Preface	iv
	Introduction	1
I.	Cross Sections	5
	Photon Interactions Considered	5
	Cross-Section Formulas	5
II.	Theory	12
III.	Calculational Procedure	15
	General Description of a History	16
	Calculation of the Probabilities, Fluxes, and Dose Rates	17
	Generation of a History	24
IV.	Analysis	32
	Comparison of the Monte Carlo Solution with the Analytic Solution of the Energy Independent Boltzmann Equation	32
	Accuracy of the Singly Scattered Flux for a Beam Angle of 1 Deg	34
	Statistical Fluctuations	34
	Results	38
App. A.	List of Tables	65
App. B.	List of Figures	66

INTRODUCTION

A knowledge of the energy and angular distribution of gamma rays which escape from a source into the air is always of importance in the design of experiments involving radiation. In the past various attempts have been made to calculate, for specific point source--point detector distances, the flux resulting from air-scattered gamma rays. Because it has long been recognized that the total scattered flux at a point in air is in most cases largely made up of gamma rays that scatter only once before reaching that point, the flux resulting from gamma rays that have undergone multiple collisions always has been ignored. But for accurate interpretation of radiation experiments performed in air the contribution by all scattered gamma rays, including multiply scattered gamma rays, must be known. It was therefore decided to calculate the contribution to a point detector by multiply scattered gamma rays from a monoenergetic point source emitting a monodirectional beam in the x,y plane as shown in Fig. 1. This source was thus quite general, and the results of the calculations could be integrated to provide data for any specific source geometry.

Three parameters characterized the source: the energy, E_o, of the photons leaving the source; the distance, d_o, between the source and the detector; and the angle, A_o, between the beam and the source-detector axis (x axis). Six different values of E_o, six values of d_o, and seven values of A_o (see Table 1) were used to give a total of 252 possible combinations. The source and detector were considered to be in an essentially infinite medium of dry air with a density of 0.00125 g/cm^3. This medium was approximated by assuming that it consisted of 23.5 wt% oxygen and 76.5 wt% nitrogen. (A method of transforming the results to other densities has been described previously.[1])

---

1. C. D. Zerby, "Radiation Flux Transformation as a Function of Density of an Infinite Medium with Anisotropic Point Sources," ORNL-2100 (Oct. 1956).

Table 1. Numerical Values of the Source Parameters Which Were Used in the Computation

d_o (ft)	A_o (deg)	E_o (Mev)
100	1	12
65	15	7
40	30	4
20	60	2
10	90	1
5	135	0.6
	180	

d_o = source-detector separation distance.

A_o = angle between the beam of gamma rays and the source-detector axis.

E_o = energy of the photons leaving the source.

Table 2. Polar and Azimuthal Angle Intervals at the Detector

θ, Polar Angle Intervals (deg)	ϕ, Azimuthal Angle Intervals (deg)
0 - 20	0 - 45
20 - 40	45 - 90
40 - 60	90 - 135
60 - 80	135 - 180
80 - 90	
90 - 100	
100 - 120	
120 - 140	
140 - 160	
160 - 180	

UNCLASSIFIED
2-01-059-271

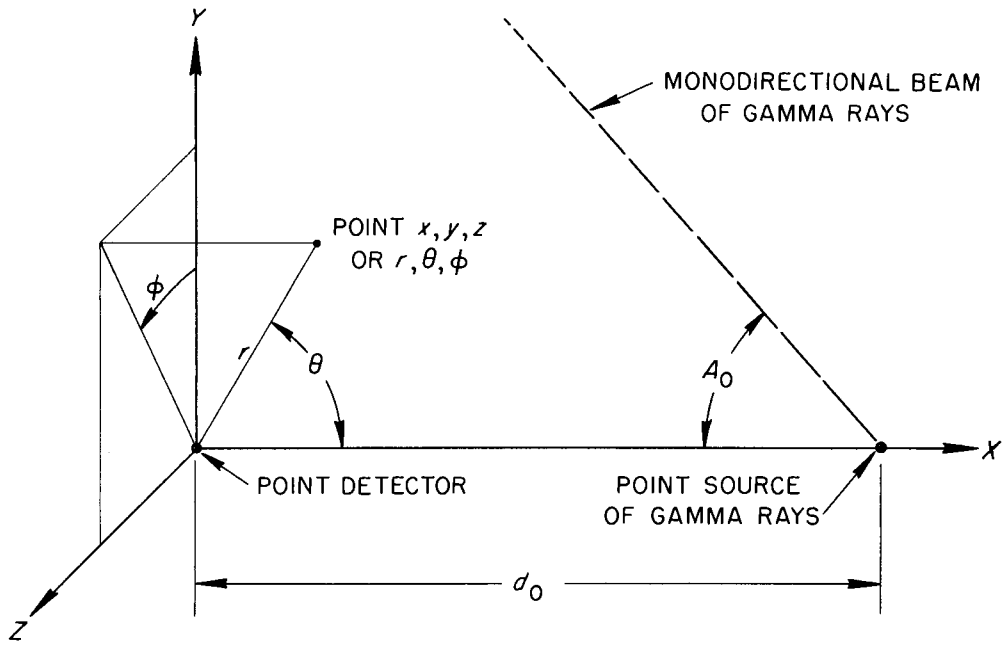

Fig. 1. Geometrical Relationship of Source and Detector.

UNCLASSIFIED
2-01-059-272

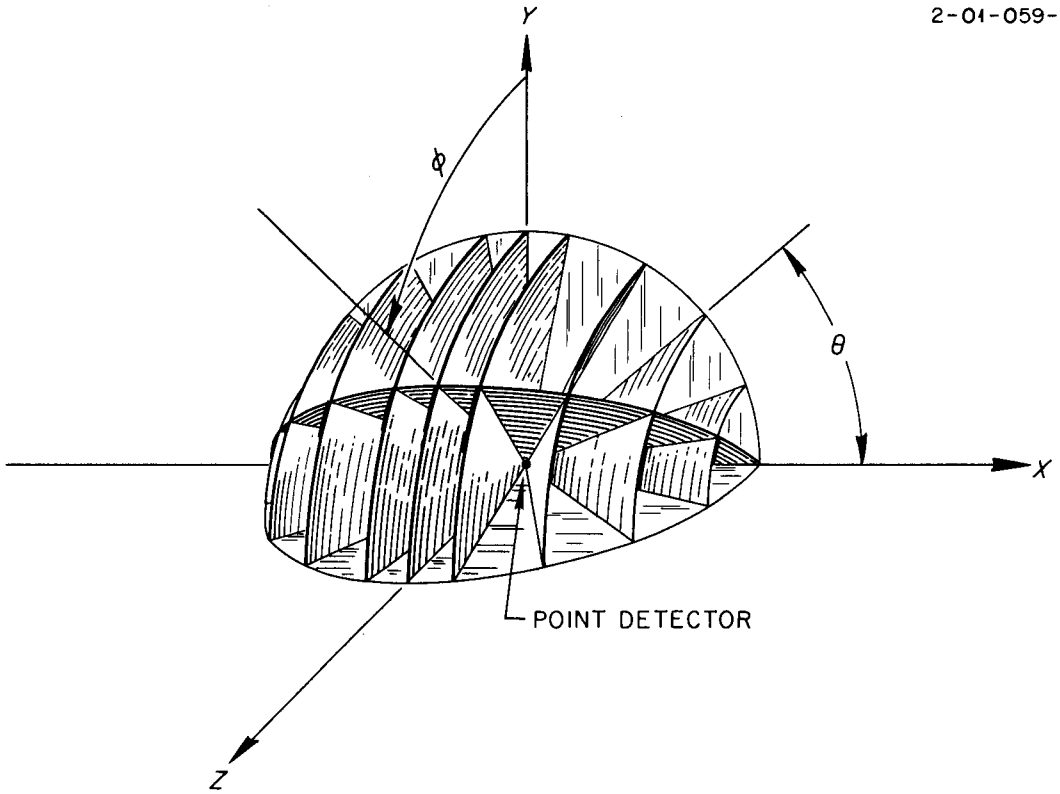

Fig. 2. The Spacial Grid System at the Detector.

The results of the calculations included the energy spectra of the flux received at the point detector and the resulting tissue dose rates.[2] In addition, the angular distribution of the flux arriving at the detector is given. In order to determine the angular distribution, the space about the detector was divided into a number of solid angles with apexes at the detector (Fig. 2). A spherical coordinate system was used, with the polar angle θ measured from the positive x axis and the azimuthal angle ϕ measured from the positive y axis in the y,z plane. The solid angles were formed by dividing the 0 - π range of θ and the 0 - π range of ϕ into the intervals listed in Table 2.*

The techniques available for calculating the mutiply scattered contributions are rather limited, particularly for the type of source chosen. The only practical technique available is the Monte Carlo method which was the method chosen. It is the purpose of this volume (volume 1) to describe the theory and the technique of the computation and to summarize the results. The results are presented in detail in volumes 2 through 5. In particular the flux data are tabulated in volumes 2 and 3 and the dose-rate data in volumes 4 and 5.

At the beginning of each of the volumes 2 through 5 is a detailed Index to the Problems which indicated where the results for any set of parameters can be located. It is to be noted that the page numbering is consecutive throughout volumes 4 and 5. By using this scheme, the flux data appearing on a particular page in volume 2 correspond to the dose-rate data appearing on the same page in volume 4. Volumes 3 and 5 have the same correspondence.

Only 50 copies of volumes 2 through 5 have been printed, some of which have been forwarded to persons known to be interested in the problem. Copies of these volumes will also be made available to other persons upon request.

---

2. The conversion factors were obtained from TID-7004, "Reactor Shielding Design Manual," T. Rockwell, editor, Office of Technical Service, Dept. of Commerce, Washington 25, D. C. (1956)

* The flux is symmetric with respect to the x,y plane, since both the source beam and the detector lie in that plane. Therefore, only values of ϕ between 0 and π need be considered for angular distribution.

I. CROSS SECTIONS

Photon Interactions Considered

Of the several different processes by which photons interact with matter, only the electron photoelectric, the atomic and electron pair-production, and the Compton scattering interactions have been taken into account in these calculations. In either the photoelectric or the pair interaction the photon is absorbed. In the Compton interaction it is deflected and loses energy. It has been shown that the other interaction processes give negligible contributions to a calculation such as described in this report.[3] For example, nuclear photoelectric effect, nuclear resonance and Thompson scattering, and Delbruck scattering have insignificant cross sections compared to the three processes retained in the investigation.[4] It can also be shown that all secondary radiation such as Bremsstrahlung, fluorescence and annihilation radiation will have little effect on this type of problem[3] and therefore can be ignored.

Cross-Section Formulas

The cross sections required in the computation are: Σ_t, the total macroscopic cross section of air (cm^{-1}); σ_t, the total average microscopic cross section for a gamma ray interacting with an electron by any of the three interaction processes considered (cm^2/electron); and σ_c, the microscopic cross section for a gamma ray interacting with an electron by the Compton scattering process alone (cm^2/electron). The ratio σ_c/σ_t is the probability that a Compton interaction occurs given that some kind of interaction does occur. Σ_t is equal to $\rho\sigma_t$, where ρ is the electron density (electrons/cm^3) of air.

---

3. C. D. Zerby, "Transmisson of Obliquely Incident Gamma Radiation through Stratified Slab Barriers," ORNL-2224, Vol. 1, p. 9-15 (Nov. 29, 1956).

4. H. A. Bethe and J. Ashkin, "Penetration of Gamma Rays," Experimental Physics, E. Segre, Editor, Vol. 1, Part II-3, pp. 345-349, John Wiley and Sons Inc., New York, 1953.

σ_c is given by the well-known Klein-Nishina formula:

$$(1) \quad \sigma_c = \pi r_e^2 \left[\frac{4(1 + E)^2(1 + 2E) - 2E^2(1 + 3E)}{E^2(1 + 2E)^2} + (E^2 - 2E - 2) \ln(1 + 2E) \right]$$

where r_e is the classical electron radius, and E is the energy of the photon. Replacing E with 1/n and simplifying the expression gives

$$(2) \quad \sigma_c = \pi r_e^2 \left[\frac{2n + 18n^2 + 16n^3 + 4n^4}{(2 + n)^4} + (n - 2n^2 - 2n^3) \ln\left(\frac{2 + n}{n}\right) \right]$$

or

$$(3) \qquad \sigma_c = \pi r_e^2 K(n)$$

where the quantity in brackets of Eq. 2 is replaced by K(n) in Eq. 3. Hastings[5] gives a rational function approximation for K(n):

$$(4) \qquad K(n) \approx K^*(n) = \frac{c_1 \xi + c_2 \xi^2 + c_3 \xi^3}{1 + d_1 \xi + d_2 \xi^2 + d_3 \xi^3}$$

where

$\xi = n/(p + n)$, for $0 \leq n < \infty$,

$p = 0.222037$,

$c_1 = 1.651035$,

$c_2 = 9.340220$,

$c_3 = 8.325004$,

---

5. Cecil Hastings, "Approximations for Digital Computers," RAND Report, R-264, p. 154 (1954); also published by Princeton University Press, 1955.

$d_1 = 12.501332,$
$d_2 = -14.200407,$
$d_3 = 1.699075.$

The error, $K^*(n) - K(n)$, is no greater than 0.001 for all n. For machine computation it is better to replace ξ with $1/\beta$ so that Eq. 4 then becomes

$$K(n) \approx K^*(n) = \frac{c_1\beta^2 + c_2\beta + c_3}{\beta^3 + d_1\beta^2 + d_2\beta + d_3} \tag{5}$$

where $\beta = (p + n)/n$. In terms of energy,

$$\beta = 1 + pE \tag{6}$$

For a given energy, σ_c was computed by using

$$\sigma_c = \pi r_e^2 K^*(n) \tag{7}$$

The photoelectric and pair production cross sections for nitrogen and oxygen are listed in a table prepared by G. White.[6] The cross sections for the photoelectric and pair production processes, together with the Compton cross section, are combined to give the total microscopic cross section in air, σ_t, assuming that the air medium consists of 23.5% oxygen and 76.5% nitrogen.

The ratio σ_t/σ_c was determined for the range of energy used in the problem, 0.01 Mev to 12 Mev.

It was convenient to split the energy range into three regions:

(1) Low energy: 0.01 to 0.216 Mev. The photoelectric effect predominates; σ_c/σ_t is an increasing function of energy.

(2) Intermediate energy: 0.216 to 1.423 Mev. Both the photoelectric effect and the pair production are negligible compared to the Compton scattering: σ_c/σ_t is equal to 1.000.

---

6. G. R. White, "X-Ray Attenuation Coefficients for 10 Kev to 100 Mev," National Bureau of Standards Report 1003 (1952).

(3) High energy: 1.423 to 12 Mev. The pair production enters; σ_c/σ_t is a decreasing function of energy.

The method of least squares was used in order to obtain a simple expression for σ_c/σ_t for the high-energy and the low-energy ranges:

$$(8) \qquad \frac{\sigma_t}{\sigma_c} = \begin{cases} A + B(1/E) + C(1/E)^2 + D(1/E)^3 & \text{for } K \leq E < L \\ 1.000 \quad \text{for } L \leq E < M \\ F + G(E) + H(E)^2 + J(E)^3 & \text{for } M \leq E < N \end{cases}$$

where

	Energy (Mev)	Energy ($m_o c^2$)
A	0.98396	0.98396
B	0.0045216	0.0088517
C	-0.00032364	-0.0012404
D	0.000020907	0.00015688
F	0.97591	0.97591
G	0.013244	0.0067649
H	0.0026846	0.00070043
J	-0.000057918	-0.000007717
K	0.01	0.01958
L	0.216	0.423
M	1.423	2.786
N	12.0	23.49

This ratio, together with Eq. 7, was used to compute the total macroscopic cross section:

$$(9) \qquad \Sigma_t = \rho\sigma_t = \rho \frac{\sigma_t}{\sigma_c} \sigma_c \approx \rho \frac{\sigma_t}{\sigma_c} \pi r_e^2 K^*(n)$$

Table 3 gives values of σ_c, Σ_t, and σ_t/σ_c which were calculated by using the above expressions; these values are compared with the data from G. White where possible. Figure 3 is a plot of Σ_t and σ_t/σ_c as a function of energy.

The angular dependence of Compton scattering was determined by the Klein-Nishina differential cross-section formula:

$$(10) \qquad \frac{d\sigma_c}{d\Omega} = \frac{r_e^2}{2} \left(\frac{E'}{E}\right)^2 \left(\frac{E'}{E} + \frac{E}{E'} - \sin^2\theta\right)$$

Table 3. Computed Values of Σ_t, σ_t/σ_c, and σ_c

Energy		$\Sigma_t = \rho\ \sigma_t$	σ_t/σ_c			σ_c (barns/electron)		
Mev	$m_o c^2$	$(cm)^{-1}$ (a)	Computed	G-W[b]	% Error	Computed	G-W	% Error
0.015	0.029	0.00140154	6.0415	6.0331	0.139	0.62859	0.62700	0.253
0.020	0.039	0.00068708	3.0144	3.0202	0.192	0.61761	0.61600	0.261
0.030	0.059	0.00034145	1.5494	1.5602	0.695	0.59713	0.59600	0.190
0.040	0.078	0.00026073	1.2214	1.2208	0.046	0.57842	0.57800	0.073
0.050	0.098	0.00023037	1.1122	1.1087	0.312	0.56124	0.56100	0.043
0.060	0.117	0.00021462	1.0662	1.0610	0.491	0.54541	0.54600	0.107
0.070	0.137	0.00020440	1.0435			0.53078		
0.080	0.157	0.00019674	1.0307	1.0254	0.517	0.51719	0.51700	0.036
0.090	0.176	0.00019047	1.0229			0.50454		
0.100	0.196	0.00018507	1.0177	1.0130	0.462	0.49274	0.49290	0.033
0.150	0.294	0.00016471	1.0059	1.0038	0.212	0.44368	0.44360	0.018
0.200	0.392	0.00015020	1.0011	1.0007	0.037	0.40653	0.40660	0.017
0.300	0.587	0.00013054	1.0000	1.0000	0.000	0.35370	0.35350	0.058
0.400	0.783	0.00011690	1.0000	1.0000	0.000	0.31675	0.31670	0.017
0.500	0.979	0.00010671	1.0000	1.0000	0.000	0.28915	0.28920	0.017
0.600	1.175	0.00009871	1.0000	1.0000	0.000	0.26746	0.26750	0.015
0.700	1.370	0.00009219	1.0000			0.24979		
0.800	1.566	0.00008672	1.0000	1.0000	0.000	0.23499	0.23500	0.005
0.900	1.762	0.00008206	1.0000			0.22234		
1.000	1.958	0.00007800	1.0000	1.0000	0.000	0.21134	0.21120	0.068
1.500	2.937	0.00006347	1.0016	1.0018	0.018	0.17170	0.17160	0.056
2.000	3.916	0.00005476	1.0127	1.0082	0.445	0.14652	0.14640	0.079
3.000	5.873	0.00004411	1.0382	1.0324	0.566	0.11512	0.11510	0.016
4.000	7.831	0.00003779	1.0681	1.0632	0.464	0.09586	0.09600	0.150
5.000	9.789	0.00003362	1.1020	1.1015	0.046	0.08266	0.08280	0.175
6.000	11.747	0.00003069	1.1395	1.1425	0.264	0.07298	0.07320	0.305
7.000	13.704	0.00002855	1.1803			0.06554		
8.000	15.662	0.00002694	1.2240	1.2285	0.364	0.05964	0.05990	0.438
9.000	17.620	0.00002570	1.2703			0.05482		
10.000	19.578	0.00002473	1.3189	1.3229	0.305	0.05080	0.05100	0.386
12.000	23.493	0.00002380	1.4213					
0.015	0.029	0.00140154	6.0415	6.0331	0.139	0.62859	0.62700	0.253
0.020	0.039	0.00068708	3.0144	3.0202	0.192	0.61761	0.61600	0.261
0.030	0.059	0.00034145	1.5494	1.5602	0.695	0.59713	0.59600	0.190
0.040	0.078	0.00026073	1.2214	1.2208	0.046	0.57842	0.57800	0.073
0.050	0.098	0.00023037	1.1122	1.1087	0.312	0.56124	0.56100	0.043
0.060	0.117	0.00021462	1.0662	1.0610	0.491	0.54541	0.54600	0.107
0.070	0.137	0.00020440	1.0435			0.53078		
0.080	0.157	0.00019674	1.0307	1.0254	0.517	0.51719	0.51700	0.036
0.090	0.176	0.00019047	1.0229			0.50454		
0.100	0.196	0.00018507	1.0177	1.0130	0.462	0.49274	0.49290	0.033
0.150	0.294	0.00016471	1.0059	1.0038	0.212	0.44368	0.44360	0.018
0.200	0.392	0.00015020	1.0011	1.0007	0.037	0.40653	0.40660	0.017
0.300	0.587	0.00013054	1.0000	1.0000	0.000	0.35370	0.35350	0.058
0.400	0.783	0.00011690	1.0000	1.0000	0.000	0.31675	0.31670	0.017
0.500	0.979	0.00010671	1.0000	1.0000	0.000	0.28915	0.28920	0.017
0.600	1.175	0.00009871	1.0000	1.0000	0.000	0.26746	0.26750	0.015
0.700	1.370	0.00009219	1.0000			0.24979		
0.800	1.566	0.00008672	1.0000	1.0000	0.000	0.23499	0.23500	0.005
0.900	1.762	0.00008206	1.0000			0.22234		
1.000	1.958	0.00007800	1.0000	1.0000	0.000	0.21134	0.21120	0.068
1.500	2.937	0.00006347	1.0016	1.0018	0.018	0.17170	0.17160	0.056
2.000	3.916	0.00005476	1.0127	1.0082	0.445	0.14652	0.14640	0.079
3.000	5.873	0.00004411	1.0382	1.0324	0.566	0.11512	0.11510	0.016
4.000	7.831	0.00003779	1.0681	1.0632	0.464	0.09586	0.09600	0.150
5.000	9.789	0.00003362	1.1020	1.1015	0.046	0.08266	0.08280	0.175
6.000	11.747	0.00003069	1.1395	1.1425	0.264	0.07298	0.07320	0.305
7.000	13.704	0.00002855	1.1803			0.06554		
8.000	15.662	0.00002694	1.2240	1.2285	0.364	0.05964	0.05990	0.438
9.000	17.620	0.00002570	1.2703			0.05482		
10.000	19.578	0.00002473	1.3189	1.3229	0.305	0.05080	0.05100	0.386
12.000	23.493	0.00002380	1.4213					

a. ρ = electron density of air = 0.0003764×10^{24} electrons/cm^3 for air density of 0.00125 g/cm^3.

b. From G. White, "X-Ray Attenuation Coefficients for 10 Kev to 100 Mev," NBS-1003 (1952).

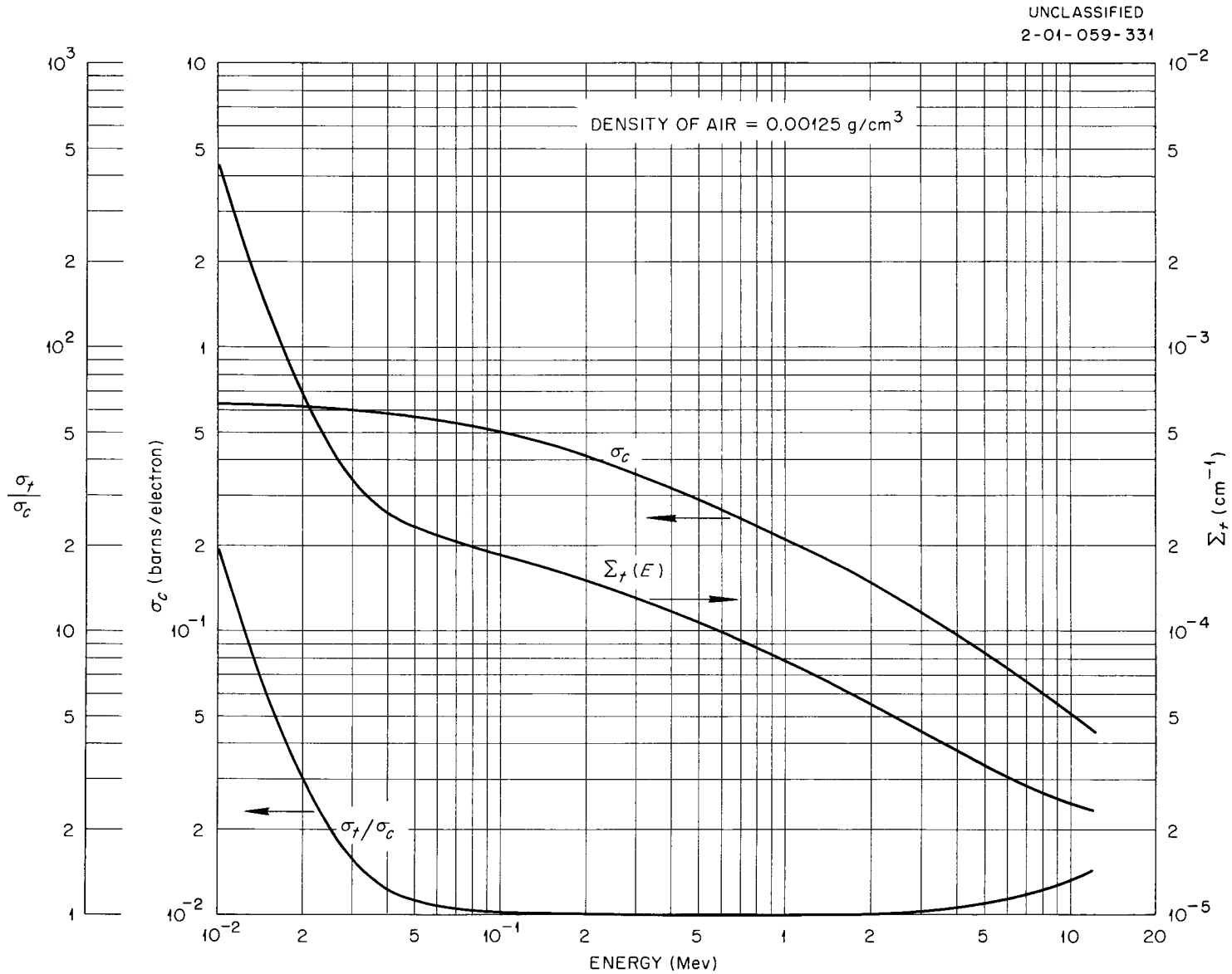

Fig. 3. Total Cross Section, Σ_t, Compton Cross Section, σ_c, and the Ratio σ_t/σ_c for Air as a Function of Energy.

where $E(m_o c^2)$ is the energy of the photon before the collision, E' is the energy of the photon after the collision, θ is the angle of deflection, r_e is the classical radius of the electron, and Ω is the solid angle into which the photon scatters. Integration of Eq. 10 over 4π steradians gives the total Compton cross section (Eq. 1). The expression:

$$\frac{1}{\sigma_c} \frac{d\sigma_c}{d\Omega} \quad d\Omega \tag{11}$$

is the probability that a photon will scatter through an angle θ into a solid angle, $d\Omega$, given that there is a Compton interaction.

Finally, the relationship between the energy of the photon before the collision and its energy after the collision is given by:

$$E' = \frac{E}{1 + E(1 - \cos\theta)} \tag{12}$$

II. THEORY

The most practical way to solve the gamma-ray air-scattering problem in the detail required is by the use of the Monte Carlo method. The particular form of Monte Carlo employed in this calculation in effect solved the Boltzmann equation in its integral form. Previous success with this technique in a similar neutron air-scattering problem[7] assured reasonable statistical accuracy.

If the detector point is taken at the origin of the coordinate system, then the integral form of the Boltzmann equation in an infinite homogeneous medium where the source beam does not point directly at the detector point is given by

$$(13) \qquad \phi(0,E,\vec{\Omega}) = \int_{\substack{\text{all}\\\text{space}}} \int_{E''} \int_{\vec{\Omega}''} \Sigma_t(E'')\phi(\vec{r}',E'',-\vec{\Omega}'') \frac{\sigma_c(E'')}{\sigma_t(E'')} f(E,E'',-\vec{\Omega},\vec{\Omega}'') \times e^{-\Sigma_t(E)r'} \frac{\delta(\vec{\Omega}',\vec{\Omega})}{r'^2} d\vec{r}'dE''d\vec{\Omega}''$$

where

$\vec{\Omega}$ = a unit vector,

$\phi(0,E,\vec{\Omega})$ = photons per cm^2 per sec per unit energy at energy E per steradian about the negative direction $-\vec{\Omega}$ at the origin,

$d\vec{r}'' = r''^2 d\vec{\Omega}''dr''$,

and

$\delta(\vec{\Omega}',\vec{\Omega}) = 0$ if $\vec{\Omega}' \neq \vec{\Omega}$,

$$\int_{\vec{\Omega}'} \delta(\vec{\Omega}',\vec{\Omega})d\vec{\Omega}' = 1.$$

The function f in Eq. 13 is associated with the differential scattering cross section by the relation

---

7. C. D. Zerby, "A Monte Carlo Calculation of Air-Scattered Neutrons," ORNL-2277 (April 23, 1957).

$$(14) \qquad f(E,E'',-\vec{\Omega},\vec{\Omega}'') = \frac{\frac{d\sigma_c}{d\Omega}(E'';-\vec{\Omega}\cdot\vec{\Omega}'',E')\delta(E'-E)}{\sigma_c(E'')}$$

where $\frac{d\sigma_c}{d\Omega}(E'';-\vec{\Omega}\cdot\vec{\Omega}'',E')$ is the differential scattering cross section for scattering from a direction $\vec{\Omega}''$ with energy E" into a unit solid angle about direction $-\vec{\Omega}$ with resulting energy E'.

Equation 13 cannot be solved by Monte Carlo as it stands; however, the quantity

$$(15) \qquad X_{e\theta\phi} = \int_{\Delta\Omega_{\theta\phi}} \int_{E_e} \Phi(0,E,\vec{\Omega})\,dE\,d\vec{\Omega}$$

can be determined. In Eq. 15 the quantity $X_{e\theta\phi}$ is the probability that a photon enters the detector through the eth energy interval, the θth polar angle interval, and the ϕth azimuthal angle interval. The range of integration in Eq. 15 is over the solid angle interval designated by subscripts θ, ϕ, $(\Delta\Omega_{\theta\phi})$ and over the energy interval designated by subscript e, (ΔE_e).

The unknown in Eq. 13 is the collision density $\Sigma_t\phi$, which was generated by an analogue Monte Carlo method described in section III of this report. The results of the analogue process consist of a set of numbers $(\vec{r}_i, W_{i-1}, E_i, \vec{\Omega}_i')$, i = 1, 2, 3 ...., where $\vec{r}_i \equiv r_i\,\vec{\Omega}_i$ is the vector position of the ith collision, and the weight W_{i-1}, the energy E_i, and the direction $\vec{\Omega}_i'$ are the values the photon had before the ith collision. The weight W_{i-1} is the probability the photon will make the ith collision provided W_o has the value one. With the set of numbers generated in the analogue technique it is possible to approximate Eq. 15 by

$$(16) \qquad X_{e\theta\phi} = \sum_i W_i \frac{d\sigma_c(E_i;-\vec{\Omega}_i\cdot\vec{\Omega}_i',E')}{d\Omega/\sigma_c(E_i)} \frac{e^{-\Sigma_t(E')r_i}}{r_i^2} Q(E',\Delta E_e)Q(\vec{\Omega}_i,\Delta\Omega_{\theta\phi})$$

where

$$Q(E',\Delta E_e) = 1 \text{ if } E' \text{ is in } \Delta E_e$$
$$= 0 \text{ otherwise,}$$

$Q(\vec{\Omega}', \Delta\Omega_{\theta\phi})$ = 1 if Ω' has a direction within the bounds of $\Delta\Omega_{\theta\phi}$
= 0 otherwise,

and

$$W_i = W_{i-1} \frac{\sigma_c(E_i)}{\sigma_t(E_i)} \tag{17}$$

With the use of Eq. 16 it is possible to get an estimate of $X_{e\theta\phi}$ from each history. In the final result $X_{e\theta\phi}$ is averaged over the estimate from every history.

The singularity that appears in Eq. 16 was eliminated by requiring the following inequality to hold:

$$\frac{\frac{d\sigma_c}{d\Omega} e^{-\Sigma_t r_i}}{\sigma_c r_i^2} \leq 1 \tag{18}$$

This, in effect, introduces the restriction that a photon cannot have a probability of passing through the detector after a scattering collision greater than one.

III. CALCULATIONAL PROCEDURE

In order to estimate the gamma-ray flux and the gamma-ray dose rate at the detector, the probability that the photon arrives at the detector was estimated and this probability was converted to flux and dose rate. The various steps in the calculation can be discussed in terms of a gamma-ray history.

The probability density functions which govern the life of a gamma ray are known; for example,

$$\Sigma_t(E)(e^{-x\Sigma_t(E)})\,\Delta x \tag{19}$$

is the probability that a gamma ray of energy E will interact at a point between x and $x + \Delta x$. By selecting random variables from these probability distributions, the coordinates of the collisions, the energy of the photon, and the other parameters associated with the life of a gamma ray can be computed. Thus, by operating on random variables drawn from the proper distributions, a gamma-ray history can be constructed. The probability of passing through the detector can be determined for each of the randomly generated histories. The average probability, averaged over all of the histories, is an estimate of the probability that an actual gamma ray arrives at the detector.

As described in the Introduction, the source of these calculations was always considered to be a monodirectional, monoenergetic point source of gamma rays with the beam in the x,y plane (see Fig. 1 on p. 3) and was characterized by the energy, E_o, of the emitted photons; the distance, d_o, between the source and the detector; and the angle, A_o, between the photon beam and the source-detector axis (x axis). The numerical values of these different parameters are given in Table 1 on p. 2, a calculation being performed for each of the 252 possible combinations of the values. The source and detector were assumed to be in an infinite medium of dry air,* which had a density of 0.00125 g per cc (Ref. 1). Air was approximated by using a composition of 23.5% oxygen and 76.5% nitrogen by weight. The

*Actually, the medium was not quite infinite since the photon history was terminated if the photon wandered more than 32 mean free paths from the detector.

method used for determining the cross sections for the interactions of the gamma rays in air is discussed in the preceding section of this report (section I).

In most cases the detector was considered to be a point; however, in certain parts of the computation it was necessary to treat it as a sphere with a cross-sectional area equal to 1 cm^2. In order to determine the angular distribution of the flux, the space about the point detector was divided into a number of solid angles with apexes at the detector as shown in Fig. 2 on p. 3. Using the conventional spherical coordinate system with the polar angle, θ, measured from the positive x axis in the x,y plane and the azimuthal angle, ϕ, measured from the positive y axis in the y,z plane, the solid angles were formed by dividing the 0 - π range of θ and the 0 - π range of ϕ into intervals.* These intervals are listed in Table 2 on p. 2. In order to determine the spectrum, energy intervals were formed by dividing the energy range between the source energy and the minimum energy (0.01 Mev) into 15 approximately equal logarithmic steps.

General Description of a History

At the beginning of a history, the energy of the photon and its direction are known since the source parameters are given. The distances between the source and the first collisions are determined by choosing the distances systematically from the exponential distribution. Since the direction and the energy of the photon before a collision are known and the coordinates of that collision are also known, the coordinates of the next collision can be determined by randomly selecting both the angle of deflection and the distance between collisions. Instead of randomly deciding whether the photon is scattered or absorbed, the photon is considered to always be scattered and its weight is adjusted at each collision point. The weight of the photon after the ith collision, W_i, is the fraction of the photon remaining after i collisions and is given by:

$$W_i = \prod_{k=1}^{i} \frac{\sigma_c}{\sigma_t} (E_k) \tag{19}$$

* The flux and dose rate are symmetric with respect to the x,y plane since both the source beam and the detector lie in that plane; therefore, only values of ϕ between 0 and π need be considered for the angular distribution.

where $\frac{\sigma_c}{\sigma_t}$ (E) is defined in Section I and E_k is the energy before the kth collision. The history is terminated if (1) the energy decreases below a minimum energy (0.01 Mev); (2) the distance between the collision point and the detector exceeds 32 mean free paths; or (3) the number of collisions exceeds 51.

Calculation of the Probabilities, Fluxes, and Dose Rates

Knowing the energy and direction of the photon before the collision, the coordinates of the collision point, and the weight of the photon after the collision, it is possible to calculate the probability that the photon will pass through the detector before the next collision. As indicated in Section II the following information is required for the calculation.

(1) The distance, r, between the collision point and the detector.

(2) The angle of deflection, ψ, which would turn the photon into a direction toward the detector.

(3) The energy, E', after collision (if the photon does scatter through the angle ψ).

(4) The probability, $\frac{1}{\sigma_c}\frac{d\sigma_c}{d\Omega}\Delta\Omega$, that the photon scatters through the angle ψ into the solid angle $\Delta\Omega$ subtended by the detector.*

(5) The cross section, $\sigma_t(E')$, at the energy E'.

The probability, $X_{E'\theta'\phi'in}$, that the photon passes through the detector after the ith collision but before the $i + 1^{st}$ collision of the nth history is given by:

$$X_{E'\theta'\phi'in} = \left[W_i\right]\left[\frac{1}{\sigma_c}\frac{d\sigma_c}{d\Omega}\Delta\Omega\right]\left[e^{-r\Sigma_t(E')}\right] \tag{20}$$

where $e^{-r\Sigma_t(E')}$ is the probability that the photon travels at least as far as the detector after the collision. The sucscripts E', θ', and ϕ' indicate that at the detector the photon has energy E' and is traveling in a direction with polar angle θ' and azimuthal angle ϕ'.**

*Here it was necessary to assume that the detector was a sphere of unit cross sectional area.

**The angles are given in Fig. 1, p. 3.

The quantity $X_{E'\theta'\phi'in}$ is a random variable; its probability density function depends upon the spacial distribution of collisions and the direction of the photons before collision. This probability density function is itself a function of the source parameters. With a fixed source, the generation of a history picks the collision points and the directions before the collision from the proper distribution.

Now let

$$X_{e\theta\phi n} = \sum_i X_{E'\theta'\phi'in}\, Q(\Omega', \Delta\Omega_{e\phi})Q(E',\Delta E_e) \tag{21}$$

where the subscripts e, θ, and ϕ (without primes) are integers which indicate the eth energy interval, the θth polar angle interval, and the ϕth azimuthal angle interval of the detector. The definition of the Q functions are given below Eq. 16. The summation is over all collisions of the nth history. By the law of large numbers, the average

$$X_{e\theta\phi} = \frac{1}{N}\sum_{n=1}^{N} X_{e\theta\phi n} \tag{22}$$

approaches the expected value of $X_{e\theta\phi}$ as the number of histories becomes infinite. This expected value is the probability that a photon, which leaves the specified source, passes through the detector with energy in the eth energy interval and with direction such that its polar angle and its azimuthal angle are in the θth and ϕ^{th} intervals. In addition, the quantity $X_{e\theta\phi}/\Delta E_e \Delta\cos\theta_\theta \Delta\phi_\phi$, where $\Delta\cos\theta_\theta \Delta\phi_\phi = \Delta\Omega_{\theta\phi}$, is an estimate of the <u>average</u> probability, per unit energy per steradian, of the photon entering the eth, θ^{th}, and ϕ^{th} intervals.

It is to be noted that in order to compute the incremental solid angle subtended by the detector at a collision point the cross-sectional area of the detector is taken to be 1 cm^2. Hence, $X_{e\theta\phi}/\Delta E_e \Delta\cos\theta_\theta \Delta\phi_\phi$ can be interpreted as an estimate of the average photon current at the detector with units of photons per cm^2 per unit energy per steradian per sec normalized to one source photon per sec in the eth energy interval, θ^{th} polar angle interval, and ϕ^{th} azimuthal angle interval.

Since $X_{e\theta\phi}$ can be interpreted as a gamma-ray current (photons per cm^2 per sec per source photons per sec), the dose rate due to the photons which pass through the detector with energy in the eth energy interval and with direction in the θth and ϕ^{th} angle intervals can be approximated by $T_e X_{e\theta\phi}$, where T_e is the average tissue gamma-ray dose rate with units of roentgens per hr per photons per cm^2 per sec. The value of T_e is determined for the eth energy interval by

$$T_e = \frac{\int_{\Delta E_e} T(E)dE}{\int_{\Delta E_e} dE} \tag{23}$$

For this average, the variation of dose rate as a function of energy, T(E), was assumed to be linear on a log-log plot over the interval ΔE_e for each e. Hence, the conversion factors were calculated with

$$T_e = \frac{E_e T(E_e) - E_{e+1} T(E_{e+1})}{(\beta + 1)(E_e - E_{e+1})} \tag{24}$$

where

$$\beta = \frac{\log\left[T(E_e)\right] - \log\left[T(E_{e+1})\right]}{\log(E_e) - \log(E_{e+1})}$$

In Eq. 24, E_e and E_{e+1} are the upper and lower energy bounds, respectively, of the interval ΔE_e.

Figure 4 (taken from Ref. 2) shows the relationship between tissue gamma-ray dose rate per unit photon flux as a function of energy. Table 4 lists the conversion factors which were used in the computation.

An estimate of the standard deviation of the mean of several of the probabilities was computed. The standard deviation was computed in terms of the total contribution of each of N histories, and it was computed on the mean of the probability for the N histories. For example, the standard deviation for the total detector response is given by:

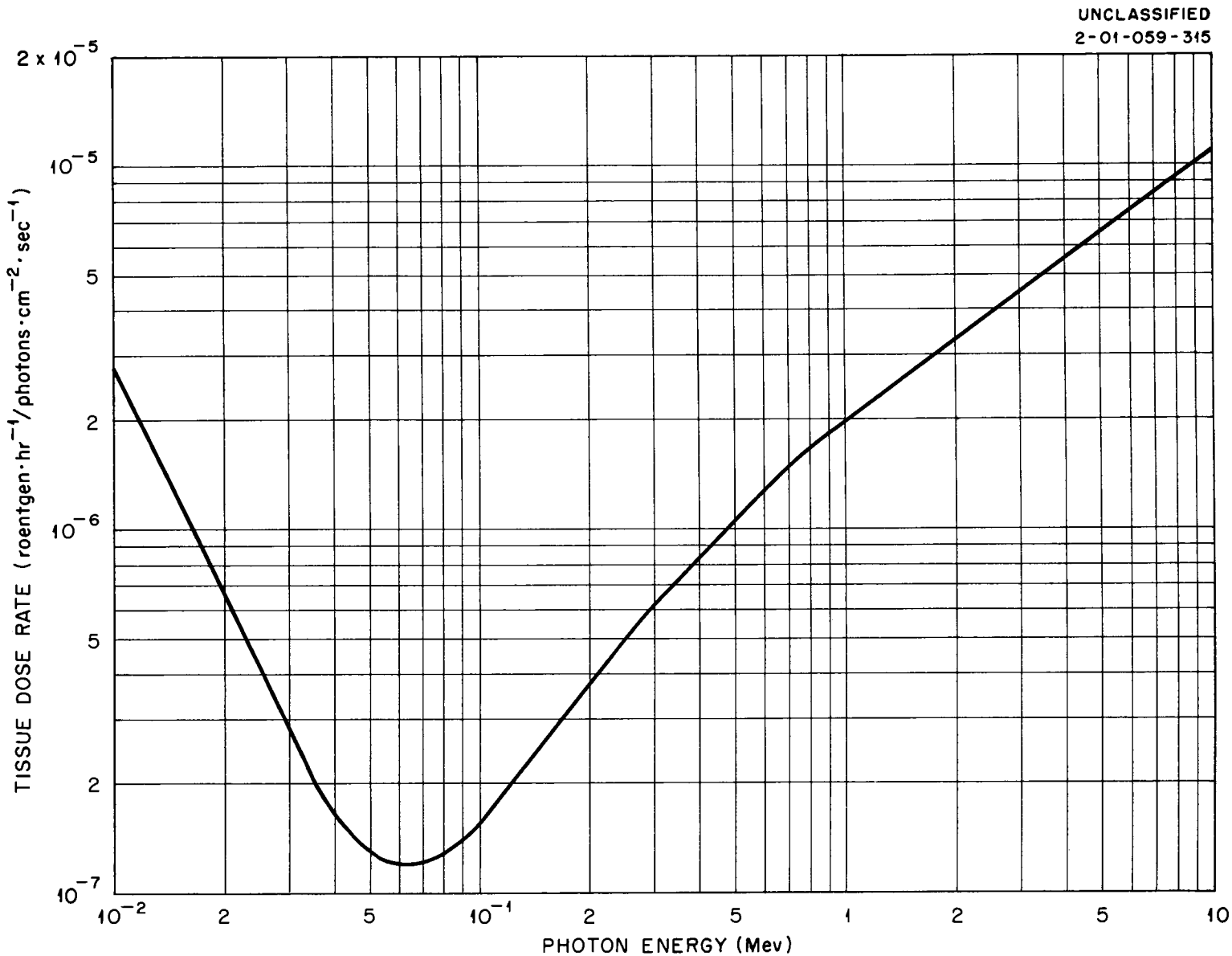

Fig. 4. Tissue Gamma-Ray Dose Rate per Unit Photon Flux as a Function of Energy (Taken from TID-7004).

Table 4. Dose-Rate Conversion Factors, T_e, for the Energy Intervals (E_e, E_{e+1}) Corresponding to Each Source Energy, E_o

e	E_e (Mev)	T_e ($r \cdot hr^{-1}/photons \cdot cm^{-2} \cdot sec^{-1}$)
	E_o = 12 Mev	
1	12.0	1.06×10^{-5}
2	7.0	6.97×10^{-6}
3	4.50	4.97×10^{-6}
4	2.75	3.51×10^{-6}
5	1.75	2.51×10^{-6}
6	1.10	1.78×10^{-6}
7	0.660	1.14×10^{-6}
8	0.400	6.58×10^{-7}
9	0.250	3.89×10^{-7}
10	0.160	2.24×10^{-7}
11	0.100	1.41×10^{-7}
12	0.064	1.41×10^{-7}
13	0.039	2.63×10^{-7}
14	0.025	6.74×10^{-7}
15	0.016	1.79×10^{-6}
	0.010	
	E_o = 7 Mev	
1	7.00	6.97×10^{-6}
2	4.50	5.06×10^{-6}
3	3.00	3.74×10^{-6}
4	1.90	2.68×10^{-6}
5	1.20	1.90×10^{-6}
6	0.800	1.33×10^{-6}
7	0.500	8.54×10^{-7}
8	0.320	5.38×10^{-7}
9	0.220	3.28×10^{-7}
10	0.140	1.89×10^{-7}
11	0.090	1.30×10^{-7}
12	0.058	1.46×10^{-7}
13	0.038	2.72×10^{-7}
14	0.025	7.35×10^{-7}
15	0.015	1.94×10^{-6}
	0.010	

Table 4. (Continued)

e	E_e (Mev)	T_e ($r \cdot hr^{-1}$/photons$\cdot cm^{-2} \cdot sec^{-1}$)
	E_o = 4 Mev	
1	4.00	4.61×10^{-6}
2	2.60	3.46×10^{-6}
3	1.80	2.61×10^{-6}
4	1.20	1.90×10^{-6}
5	0.80	1.35×10^{-6}
6	0.550	9.11×10^{-7}
7	0.350	6.04×10^{-7}
8	0.250	3.99×10^{-7}
9	0.170	2.38×10^{-7}
10	0.110	1.48×10^{-7}
11	0.074	1.27×10^{-7}
12	0.050	1.64×10^{-7}
13	0.035	3.21×10^{-7}
14	0.023	8.02×10^{-7}
15	0.015	1.94×10^{-6}
	0.010	
	E_o = 2 Mev	
1	2.00	3.00×10^{-6}
2	1.40	2.20×10^{-6}
3	1.00	1.65×10^{-6}
4	0.700	1.23×10^{-6}
5	0.500	8.44×10^{-7}
6	0.350	5.94×10^{-7}
7	0.240	3.89×10^{-7}
8	0.170	2.54×10^{-7}
9	0.120	1.67×10^{-7}
10	0.084	1.28×10^{-7}
11	0.060	1.42×10^{-7}
12	0.040	2.18×10^{-7}
13	0.030	4.38×10^{-7}
14	0.020	9.42×10^{-7}
15	0.015	1.94×10^{-6}
	0.010	
	E_o = 1 Mev	
1	1.00	1.70×10^{-6}
2	0.740	1.30×10^{-6}
3	0.550	9.66×10^{-7}
4	0.400	7.14×10^{-7}

Table 4. (Continued)

e	E_e (Mev)	T_e ($r \cdot hr^{-1}$/photons$\cdot cm^{-2} \cdot sec^{-1}$)
	E_o = 1 Mev (cont.)	
5	0.300	4.99×10^{-7}
6	0.210	3.45×10^{-7}
7	0.160	2.44×10^{-7}
8	0.120	1.70×10^{-7}
9	0.086	1.30×10^{-7}
10	0.061	1.29×10^{-7}
11	0.046	1.75×10^{-7}
12	0.034	3.00×10^{-7}
13	0.025	5.51×10^{-7}
14	0.019	1.06×10^{-6}
15	0.014	2.08×10^{-6}
	0.010	
	E_o = 0.6 Mev	
1	0.600	1.07×10^{-6}
2	0.450	8.30×10^{-7}
3	0.350	6.04×10^{-7}
4	0.250	4.35×10^{-7}
5	0.200	3.25×10^{-7}
6	0.150	2.35×10^{-7}
7	0.120	1.70×10^{-7}
8	0.090	1.30×10^{-7}
9	0.070	1.25×10^{-7}
10	0.050	1.48×10^{-7}
11	0.040	2.18×10^{-7}
12	0.030	3.71×10^{-7}
13	0.023	6.46×10^{-7}
14	0.018	1.13×10^{-6}
15	0.014	2.08×10^{-6}
	0.010	

$$\sigma\left(\frac{1}{N}\sum X_n\right) = \sqrt{\frac{1}{N^2}\left[\sum_{n=1}^{N}(X_n)^2 - \frac{1}{N}\left(\sum_{n=1}^{N} X_n\right)^2\right]} \tag{25}$$

where

$$X_n = \sum_{e}\sum_{\theta}\sum_{\phi} X_{e\theta\phi n}.$$

This summation extends over all possible values of the indicated indices.

Generation of a History

Because of the source used, all of the first collisions occurred on a straight line. In this case the spatial distribution of first collisions is given by e^{-d}, where d is the distance in mean free paths measured from the source along the beam. Instead of using a straightforward sampling technique to pick the values of d from this exponential distribution, systematic sampling was used. For a problem in which N histories were calculated, the coordinates, $(x_{1,n}, y_{1,n}, z_{1,n})$ of the first collision of the nth history were determined by the following scheme:

$$\left\{\begin{array}{ll} x_{1,1} = d_o + \frac{1}{N}\left(\frac{\alpha_o}{\Sigma_t}\right) & \\ x_{1,n} = x_{1,n-1} + \frac{1}{N-(n-1)}\left(\frac{\alpha_o}{\Sigma_t}\right) & 1 < n \leq N \\ y_{1,1} = \frac{1}{N}\left(\frac{\beta_o}{\Sigma_t}\right) & \\ y_{1,n} = y_{1,n-1} + \frac{1}{N-(n-1)}\left(\frac{\beta_o}{\Sigma_t}\right) & 1 < n \leq N \\ z_{1,n} = 0 & 1 \leq n \leq N \end{array}\right. \tag{26}$$

where α_o and β_o are the direction cosines with respect to the x and the y axes of the line along which the first collisions occur, Σ_t is the total macroscopic cross section at the source energy, the source is at $(d_o,0,0)$, the first subscript of the coordinates indicates the collision

number (here it is the first collision), and the second subscript indicates the nth history.

This scheme is derived from the systematic sampling requirement that the distance to the first collision for the nth photon, d_{1n}, should lie in the interval $(d_{1n}^{n}, d_{1n}^{n+1})$, where d_{1n}^{n} is obtained from

$$\int_{0}^{d_{1n}^{n}} e^{-x}\, dx = \frac{n-1}{N}, \quad 1 \leq n \leq N \tag{27}$$

It can be shown that the inequality

$$d_{1n}^{n} < \sum_{j=0}^{n-1} \frac{1}{N-j} < d_{1n}^{n+1} \tag{28}$$

holds for all values of n and thus provides a simple expression for d_{1n}:

$$d_{1n} = \sum_{j=0}^{n-1} \frac{1}{N-j} \tag{29}$$

This corresponds to Eqs. 26.

The distances between collisions of photons are distributed according to the probability density function e^{-d}, where d is measured in mean free paths. Distances were selected from this distribution by using the method suggested by von Neumann.[8] This technique is summarized by the schematic diagram given in Fig. 5, in which R_i is the ith random number in the interval (0,1). On the average, 4.3 random numbers are required to obtain a value of d with this method.

The random numbers which were required for the computation were obtained by the method of congruences. A sequence of numbers: Y_0, Y_1, ... was obtained as follows:

---

8. J. von Neumann, "Various Techniques Used in Connection with Random Digits," Monte Carlo Method, Applied Mathematics Series 12, A. S. Householder, editor, U. S. Government Printing Office, Washington, D. C., 1951.

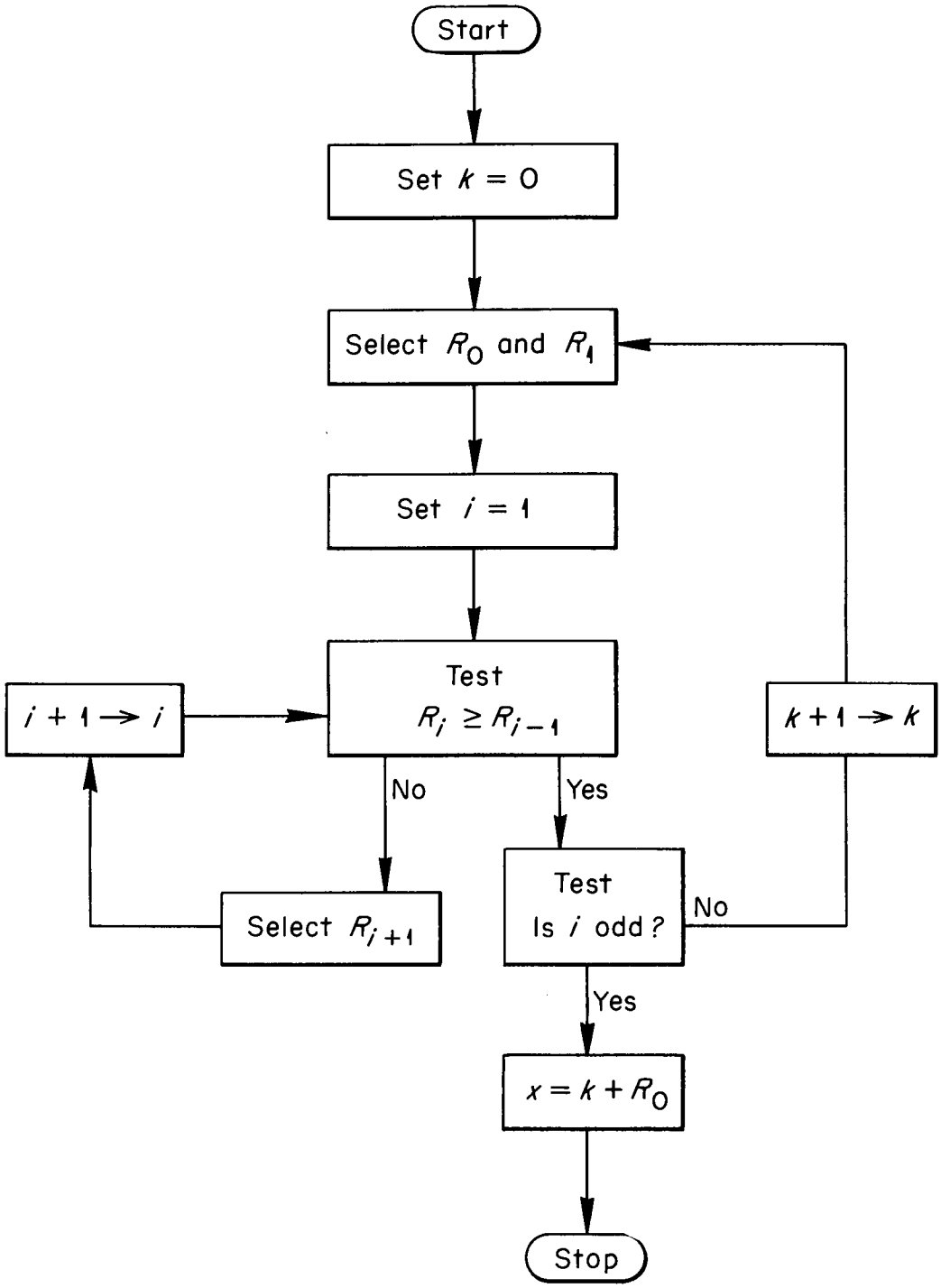

Fig. 5. Schematic Diagram of the von Neumann Method of Selecting a Random Variable x from the Probability Density Function $f(x) = e^{-x}$ where $0 \leq x < \infty$.

$$(30) \qquad \begin{cases} Y_0 = (5)^{15} \\ Y_1 = 1 \\ Y_i = (Y_0 Y_{i-1}) \bmod 2^{35}, \quad i = 2,3, \ldots \end{cases}$$

If the ith random number has the distribution

$$(31) \qquad f(R) = \begin{cases} 0, & R \leq 0 \\ 1, & 0 < R \leq 1 \\ 0, & 1 \leq R \end{cases}$$

then

$$(32) \qquad R = (Y_i) \times 2^{-35}$$

In some of the sampling techniques to be discussed it was necessary to have the random numbers in the interval (-1,1). In this case the ith random number has the distribution

$$(33) \qquad f(R) = \begin{cases} 0, & R \leq -1 \\ \frac{1}{2}, & -1 < R \leq 1 \\ 0, & 1 < R \end{cases}$$

for which

$$(34) \qquad R = (-1)^a (Y_i) \times 2^{-35}$$

where

$$a = 0 \text{ if } (Y_0 Y_{i-1}) \bmod 2^{36} < 1 \times 2^{35},$$

$$a = 1 \text{ if } (Y_0 Y_{i-1}) \bmod 2^{36} \geq 1 \times 2^{35}.$$

The number $(5)^{15}$ which is used for Y_0 is the largest odd power of 5 that does not exceed $2^{35}-1$, the largest positive integer that the

1103 computer can hold in a storage register. It can be shown[9] that 2^{33} values of Y_i can be generated before there is a repetition. The distribution and the randomness of the values of Y_i were tested using the same tests as those employed by Cameron.[9] The results of the tests indicated that the sequence of the values of Y_i was an adequate set of pseudo random numbers.

During the testing of the program it was noticed that when one problem (for E_o = 7 Mev, A_o = 90 deg, and d_o = 65 ft) was recomputed using different random numbers, the statistical fluctuation of the results from case to case was quite large. The change in direction of the photon at the points of collision was selected directly from the Klein-Nishina distribution of these cases. Since the source-detector separation was small compared to one mean free path and since scattering was predominantly forward at 7 Mev, it was reasoned that the photons were carried very far away from the detector in the first few collisions and that few of them were returning to the region around the detector. Since the contribution due to photons in this region is relatively large, the large statistical fluctuations were attributed to poor sampling in this region. When a bias sampling technique was tried, the statistical fluctuations decreased considerably and the answers for the biased case agreed within statistical error with the unbiased case. As a result, it was decided that biasing would be used for all problems. The biasing consisted of selecting the directions from the isotropic distribution and then modifying the weight of the photon to correct for sampling from the wrong distribution.

Although the selection of a direction from the Klein-Nishina differential scattering cross section distribution,

$$\frac{1}{\sigma_c} \frac{d\sigma_c}{d\Omega}$$

would have been preferable, the direction was picked from the isotropic

---

9. J. M. Cameron, Monte Carlo Experiments in SEAC, National Bureau of Standards, Statistical Engineering Laboratory, Working Paper SEL-52-5 (1951); see also Olga Taussky and John Todd, "Generation and Testing of Pseudo-Random Numbers," Symposium on Monte Carlo Methods, pp. 15-28, John Wiley, 1956.

distribution, $1/4\pi$. The resulting wrong distribution is compensated for by multiplying the weight of the photon by the ratio of the two distributions,

$$\frac{\frac{1}{\sigma_c}\frac{d\sigma_c}{d\Omega}}{\frac{1}{4\pi}}$$

where the numerator is evaluated for the direction selected from the isotropic distribution. This is justified in the following manner: Consider a fixed solid angle $\Delta\Omega$ about the direction $\vec{\Omega}$. Suppose that a very large number of directions were chosen from the isotropic distribution. Then the fraction of these which lie within the incremental solid angle is just $1/4\pi$; however, the fraction that should lie in this solid angle is

$$\frac{1}{\sigma_c}\frac{d\sigma_c}{d\Omega}\Delta\Omega$$

Multiplying the weight of the photon by the ratio changes the fraction which do enter the incremental solid angle to the correct number. For example,

$$\frac{\frac{1}{\sigma_c}\frac{d\sigma_c}{d\Omega}}{\frac{1}{4}}\left(\frac{1}{4}\Delta\Omega\right) = \frac{1}{\sigma_c}\frac{d\sigma_c}{d\Omega}\Delta\Omega \tag{35}$$

Note that the definition of "weight" has changed slightly from the definition given in Eq. 19. Henceforth, the weight will be interpreted to mean the fraction of photons which leave the collision. At the ith collision the ratio of the number of photons leaving to the number of photons entering a collision site is given by:

$$\frac{\text{Number entering}}{\text{Number leaving}} = \left(\frac{\sigma_c}{\sigma_t}\right)\left(\frac{\frac{1}{\sigma_c}\frac{d\sigma_c}{d\Omega}}{\frac{1}{4\pi}}\right) \tag{36}$$

The weight after the ith collision is given by:

$$w_i = w_{i-1} \left(\frac{\sigma_c}{\sigma_t}\right)\left(\frac{\frac{1}{\sigma_c}\frac{d\sigma_c}{d\Omega}}{\frac{1}{4\pi}}\right), \quad w_o = 1 \tag{37}$$

Since only the direction cosines of the direction of the photon after a collision were required in the computation, three direction cosines, α, β, and γ were chosen such that the direction represented by them was from the isotropic distribution. The method is schematically outlined in Fig. 6, where R_1 is a random number in the interval (0,1). R_2 and R_3, however, are random numbers in the interval (-1,1). The technique of obtaining $\cos\xi$ and $\sin\xi$ where ξ is uniformly distributed in the interval $(0,2\pi)$ was suggested by von Newmann.[8] It will be noted that in this method the test asks whether or not the point (R_2, R_3) lies inside the unit circle; if it does, the sine and cosine of twice the angle between the R_2 axis and the line joining the origin and point (R_2, R_3) is computed. It will be observed that by using twice this angle, the computation of a square root is avoided. The equations for obtaining the direction cosines are included in Fig. 6.

Once the new direction is known, the deflection from the direction before collision is determined. From this and from the energy before collision, the energy after collision can be computed using Eq. 12.

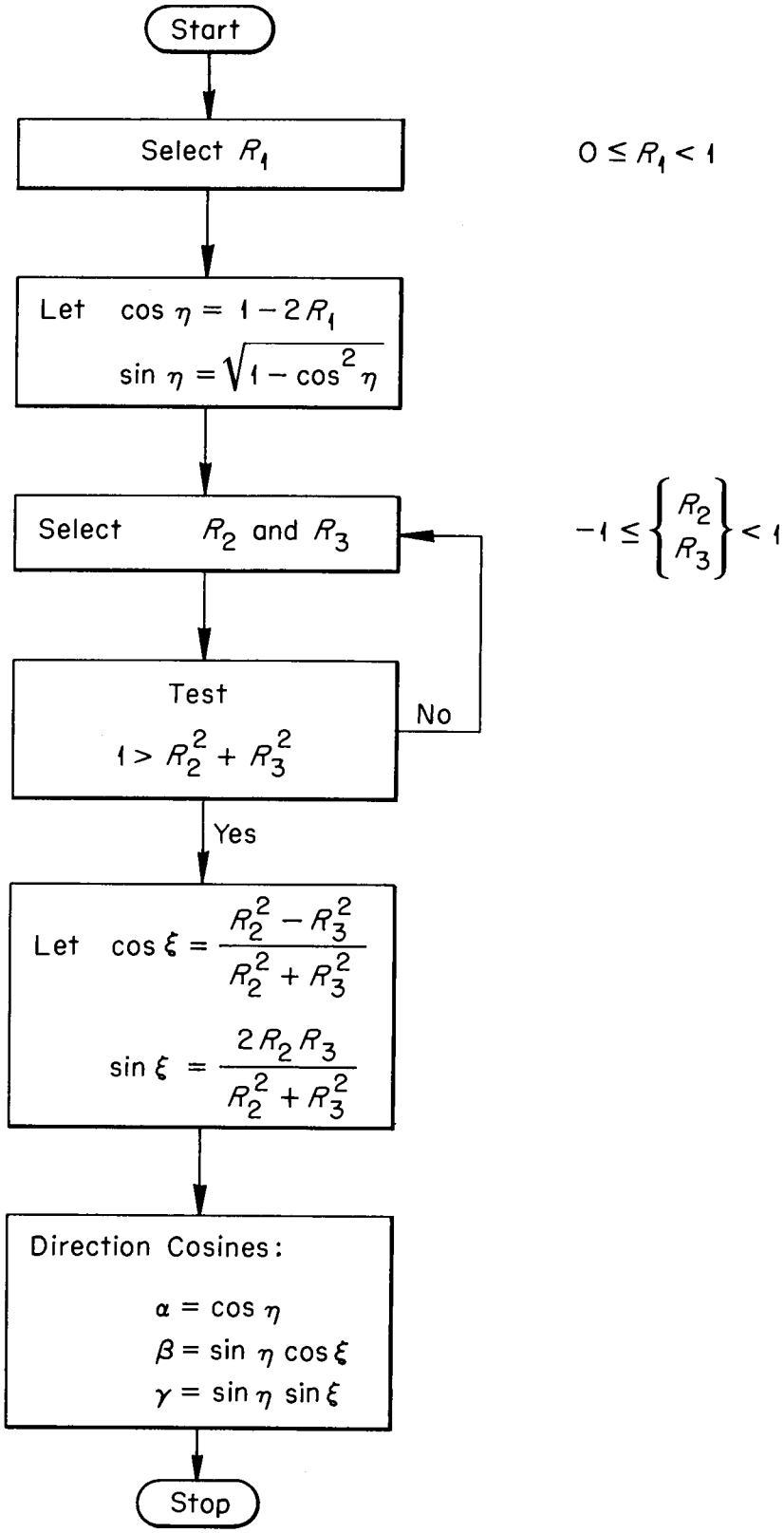

Fig. 6. Schematic Diagram of the Method of Selecting Direction Cosines from the Isotropic Distribution.

IV. ANALYSIS

Comparison of the Monte Carlo Solution with the Analytic Solution of the Energy Independent Boltzmann Equation

Analytic solutions of the Boltzmann equation giving the total flux exist only for the case of an isotropic point source in an infinite, homogeneous medium with isotropic scattering and without energy degradation. The details and results of the solutions have been given by Case, de Hoffmann, and Placzek.[10] A comparison of the analytic and Monte Carlo solutions was made by modifying the Monte Carlo calculation to use an isotropic source and to give isotropic scattering without energy degradation. The results shown in Fig. 7 are for photons which have made at least one collision, that is, the results do not include the direct-beam contribution. The solid curve represents the analytic solution while the points are the results of the Monte Carlo calculation. In this particular set of test problems all distributions were sampled randomly.

Accuracy of the Singly Scattered Flux for a Beam Angle of 180 Deg

The first-collision points for the source beam of photons were selected systematically as discussed in Section III. The Monte Carlo method used is then essentially a numerical integration for the first-collision contribution to the flux at the detector. An analysis of the accuracy of the calculation for the first collision contribution to the detector flux was made for the particular case of a photon beam directed at 180 deg from the detector point. The analytic expression for the contribution is

$$(38) \qquad \int_{x=d_o}^{\infty} e^{-\Sigma_t(E_o)(x-d_o)} \frac{\sigma_c}{\sigma_t} \left[\frac{1}{\sigma_c} \frac{d\sigma_c}{d\Omega}\right]_{180\ \mathrm{deg}} e^{-\Sigma_t(E'x)} \Sigma_t(E_o) \frac{1}{x^2}\, dx$$

10. K. M. Case, F. deHoffmann, and G. Placzek, "Introduction to the Theory of Neutron Diffusion," U. S. Government Printing Office, 1953.

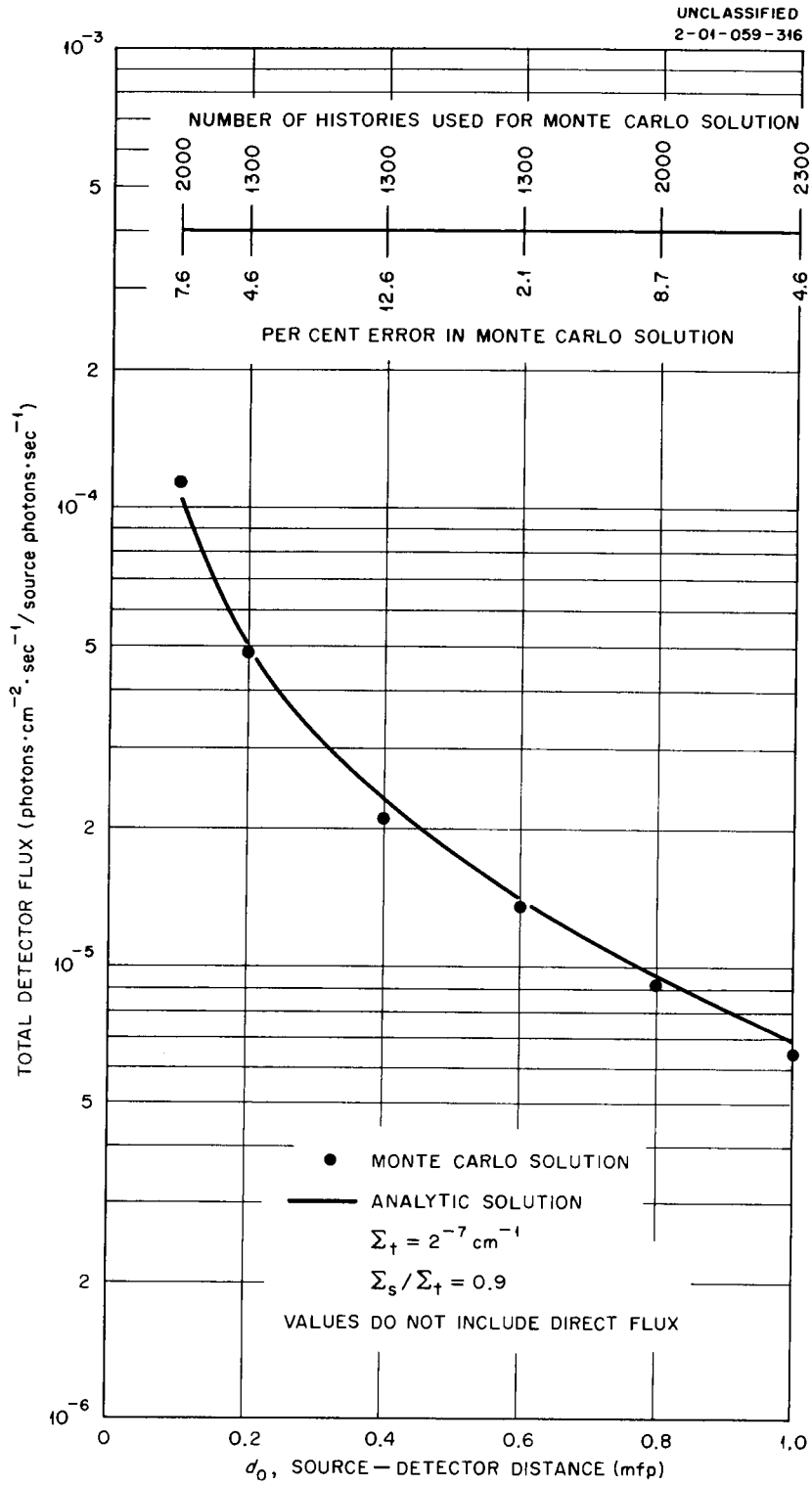

Fig. 7. Solutions of the One-Velocity Boltzmann Equation for an Isotropic Point Source of Photons in an Infinite Medium of Air.

where d_o is the source-detector separation distance, E_o is the source energy, and E' is the energy of the photon after it has turned through 180 deg. An accurate evaluation of this integral was made for several source parameters. Table 5 compares these results with the values obtained from the systematic sampling using 1800 histories. The difference between the Monte Carlo and exact solutions occur because of the approximation to the integral introduced by the systematic sampling technique described in Eq. 28.

Accuracy of the Singly Scattered Flux for a Beam Angle of 1 Deg

At a source beam angle of 1 deg the first-collision flux was found to be quite sensitive to the number of histories. Accurate computations of the first-collision flux were made by using a large number of histories. The values of the flux for those cases for which the difference is significant are tabulated in Table 6 along with the corresponding values from Volumes 2 and 3. The sensitivity of the first-collision flux contribution at a beam angle of 1 deg is attributed to the large contribution to the flux from scatterings near the detector. Since there is a large contribution from first scatterings near the detector it should be required that this region be sampled with a greater density than other regions, but this would have required special handling of the 1-deg case, and for this reason it was not done.

Statistical Fluctuations

In order to investigate the statistical fluctuation of the Monte Carlo calculation, one problem (for E_o = 7 Mev, d_o = 65 ft, and A_o = 180 deg) was run a number of times using different sets of random numbers. Figures 8 and 9 give a small portion of the results from the 18 calculations which were run. The computed values are plotted with their 95% confidence limits of $\pm$ 1.96σ. The standard deviations, σ, used in establishing these limits were the estimates* which were computed. The mean and the 95% confidence limits are also given for each set of 18 calculations in Figs. 8 and 9. Because of the symmetry about the x axis for the A_o = 180 deg cases, the quantity $\Sigma_{e\theta} X_{e\theta\phi} \Delta\phi$ has the same

* For example, see Eq. 27.

Table 5. First-Collision Contribution to the Flux at the Detector Resulting from a Point, Monodirectional Source of Photons at a Beam Angle of 180 deg

E_o, Source Energy (Mev)	d_o, Source-Detector Separation (ft)	First-Scattered Flux per Source Photon		Percent Error
		Monte Carlo Solution	Analytic Solution	
0.6	100	4.40×10^{-10}	4.43×10^{-10}	0.68
	65	9.51×10^{-10}	9.54×10^{-10}	0.31
	40	2.04×10^{-9}	2.04×10^{-9}	0.00
	20	5.30×10^{-9}	5.30×10^{-9}	0.00
	10	1.24×10^{-9}	1.24×10^{-9}	0.00
	5	2.71×10^{-8}	2.74×10^{-8}	1.10
7.0	100	5.89×10^{-11}	5.91×10^{-11}	0.34
	65	1.21×10^{-10}	1.22×10^{-10}	0.82
	40	2.49×10^{-10}	2.50×10^{-10}	0.40
	20	6.15×10^{-10}	6.22×10^{-10}	1.13
	10	1.38×10^{-9}	1.42×10^{-9}	2.82
	5	2.90×10^{-9}	3.07×10^{-9}	5.54
12.0	5	1.69×10^{-9}	1.82×10^{-9}	7.15

Table 6. First-Collision Contribution to the Flux at the Detector Resulting from a Point, Monodirectional Source of Photons at a Beam Angle of 1 deg

E_o, Source Energy (Mev)	d_o, Source-Detector Separation (ft)	First-Scattered Flux per Source Photon		Percent Error
		Monte Carlo Solution	Analytic Solution	
5	12.0	2.97×10^{-6}	3.23×10^{-6}	-8.05
	7.0	4.17×10^{-6}	4.21×10^{-6}	-0.95
	4.0	4.99×10^{-6}	5.46×10^{-6}	-8.61
	2.0	8.09×10^{-6}	7.37×10^{-6}	9.77
	1.0	9.27×10^{-6}	9.66×10^{-6}	-4.04
	0.6	1.17×10^{-5}	1.16×10^{-5}	0.86
10	12.0	1.64×10^{-6}	1.61×10^{-6}	1.82
	7.0	2.02×10^{-6}	2.09×10^{-6}	-3.35
	4.0	2.76×10^{-6}	2.71×10^{-6}	1.85
	2.0	3.64×10^{-6}	3.65×10^{-6}	-0.27
	1.0	4.75×10^{-6}	4.76×10^{-6}*	-0.21
	0.6	5.66×10^{-6}	5.68×10^{-6}**	-0.35

* 6,000 histories.

** 4,000 histories.

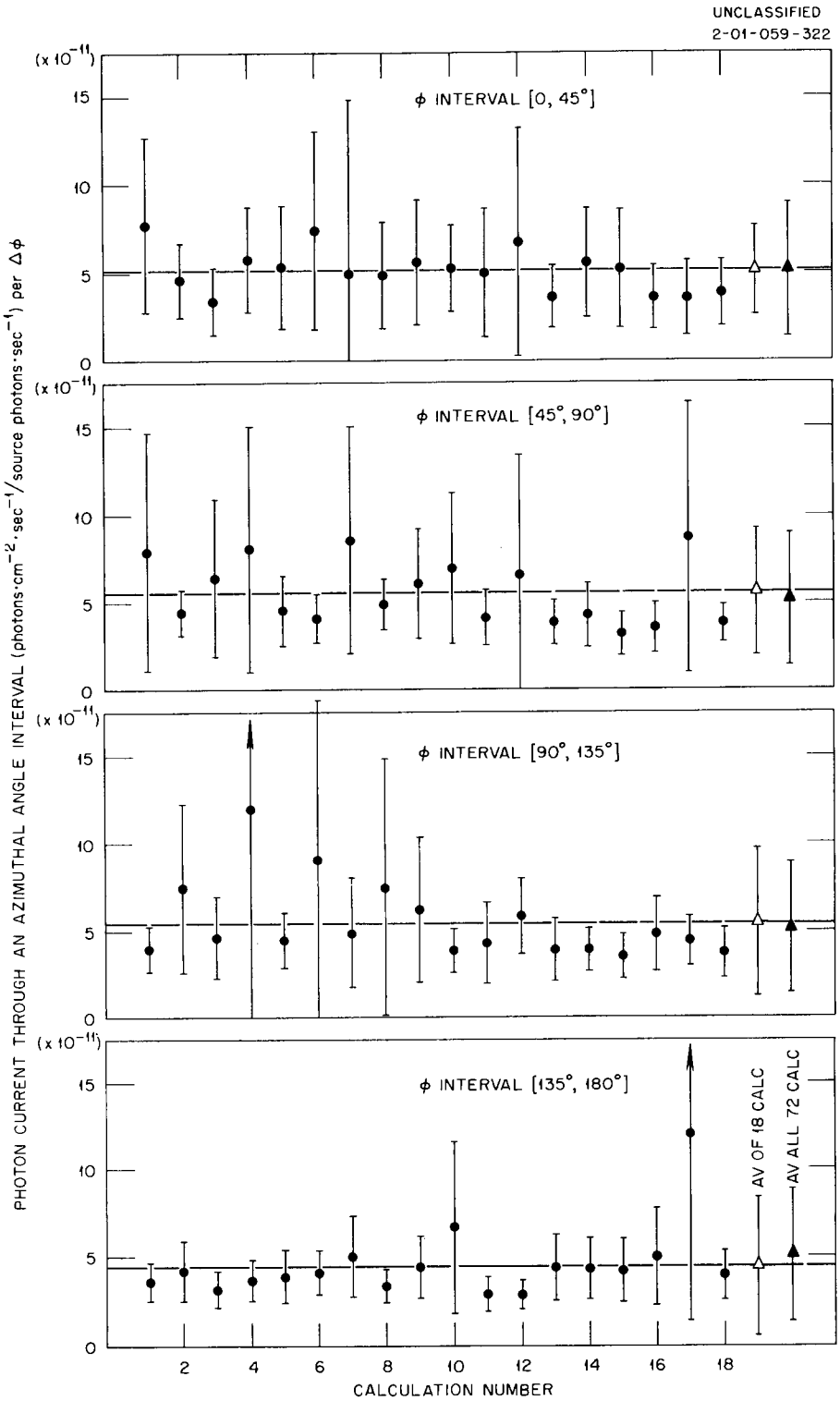

Fig. 8. Comparison of Some of the Results of 18 Different Calculations of Case 213: Photon Current Through Various Azimuthal Angle Intervals.

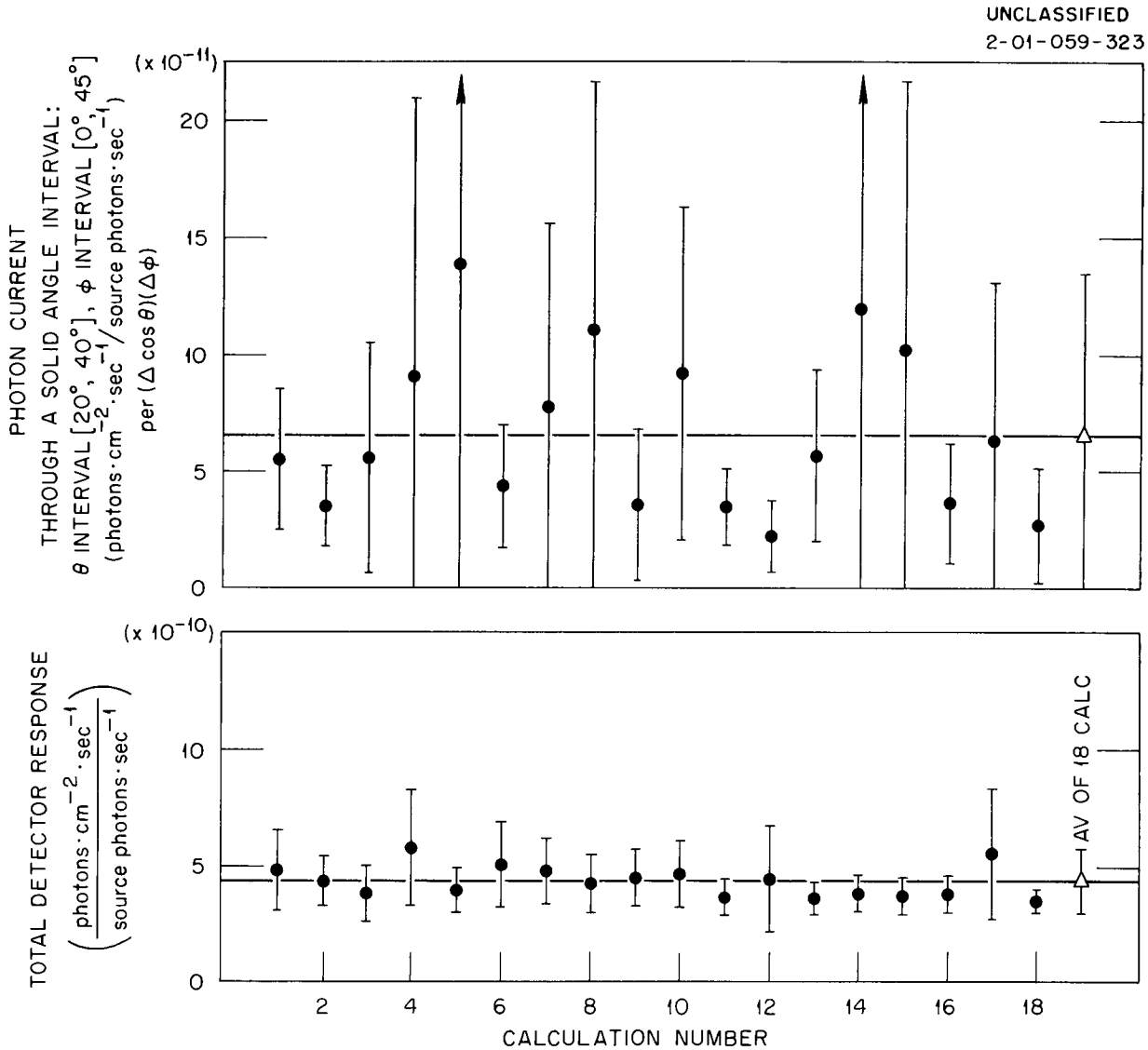

Fig. 9. Comparison of Some of the Results of 18 Different Calculations of Case 213: Photon Current Through a Solid Angle Interval and Total Detector Response.

expected value for the four different azimuthal angle intervals. The mean and the 95% confidence limits of the 72 estimates of this quantity are given in Fig. 8. An examination of both Figs. 8 and 9 seem to indicate that the standard deviation can be used to determine confidence limits on the computed estimates of the fluxes.

Results

In order to obtain a more accurate set of results, some of the cases were run more than once using different random numbers. A large number of graphs were plotted as a control on the computation. It was hypothesized that plots of flux versus the source parameters (d_o, A_o, and E_o) would yield smooth curves. If the results of any problem showed a marked deviation from the hypothesis, the case was rerun. The control graphs were plots of:

(1) $\sum_{\phi}\sum_{\theta}\sum_{e} X_{e\theta\phi}$ versus $\left\{\begin{matrix}(a) & d_o \\ (b) & E_o\end{matrix}\right\}$ log-log plots

(2) $\sum_{\theta}\sum_{e} X_{e\theta\phi}/\Delta\phi$ versus $\left\{\begin{matrix}(a) & d_o \\ (b) & E_o \\ (c) & A_o\end{matrix}\right\}$ semilog plots

(3) $\left(\dfrac{\text{First-Collision Flux}}{\text{Total Detector Response}}\right)$ X 100 versus $\left\{\begin{matrix}(a) & d_o \\ (b) & E_o \\ (c) & A_o\end{matrix}\right\}$ semilog plots

The term $\sum_{\phi}\sum_{\theta}\sum_{e} X_{e\theta\phi}$ represents the total detector response (flux), and $\sum_{\theta}\sum_{e} X_{e\theta\phi}/\Delta\phi$ is the flux entering the detector through a particular ϕ interval. For the latter graphs, the second, the third, and the fourth ϕ intervals were all plotted and in some cases the first ϕ interval was also plotted. The percent of total flux which is due to first collisions is given by (3).

After all of the results were plotted, each case, for a particular set of input parameters, was checked to see how well its results agreed with neighboring points on each of the appropriate graphs. (Note that there were 14 curves for each comparison.) By taking into account all of the data available, the trends for the different curves became apparent and the best of the data was selected for publication.

A small number of these curves are included in this report. Figures 10 through 15 show the variation of total detector response (flux) as a function of d_o for constant E_o and A_o, while Figs. 16 through 21 show the same information as a function of E_o for constant d_o and A_o. The values plotted are those which appear in Volumes 2 and 3 of this report, except for the $A_o = 1$ deg case, for which the values listed in column 4 of Table 6 were used. Figures 22 through 27 show the variation of the percent total detector response due to first collision as a function of A_o for constant E_o and d_o.

In addition, Fig. 28 shows the relationship between total detector response, first-collision flux, and multiple-collision flux as a function of d_o, for $E_o = 7$ Mev and $A_o = 180$ deg. This plot also shows the flux for d_o equal to 400 and 1000 ft.

Figures 29 through 34 show the variation of the tissue dose rate as at function of d_o for constant E_o and A_o. These data appear in volumes 4 and 5 of this report.

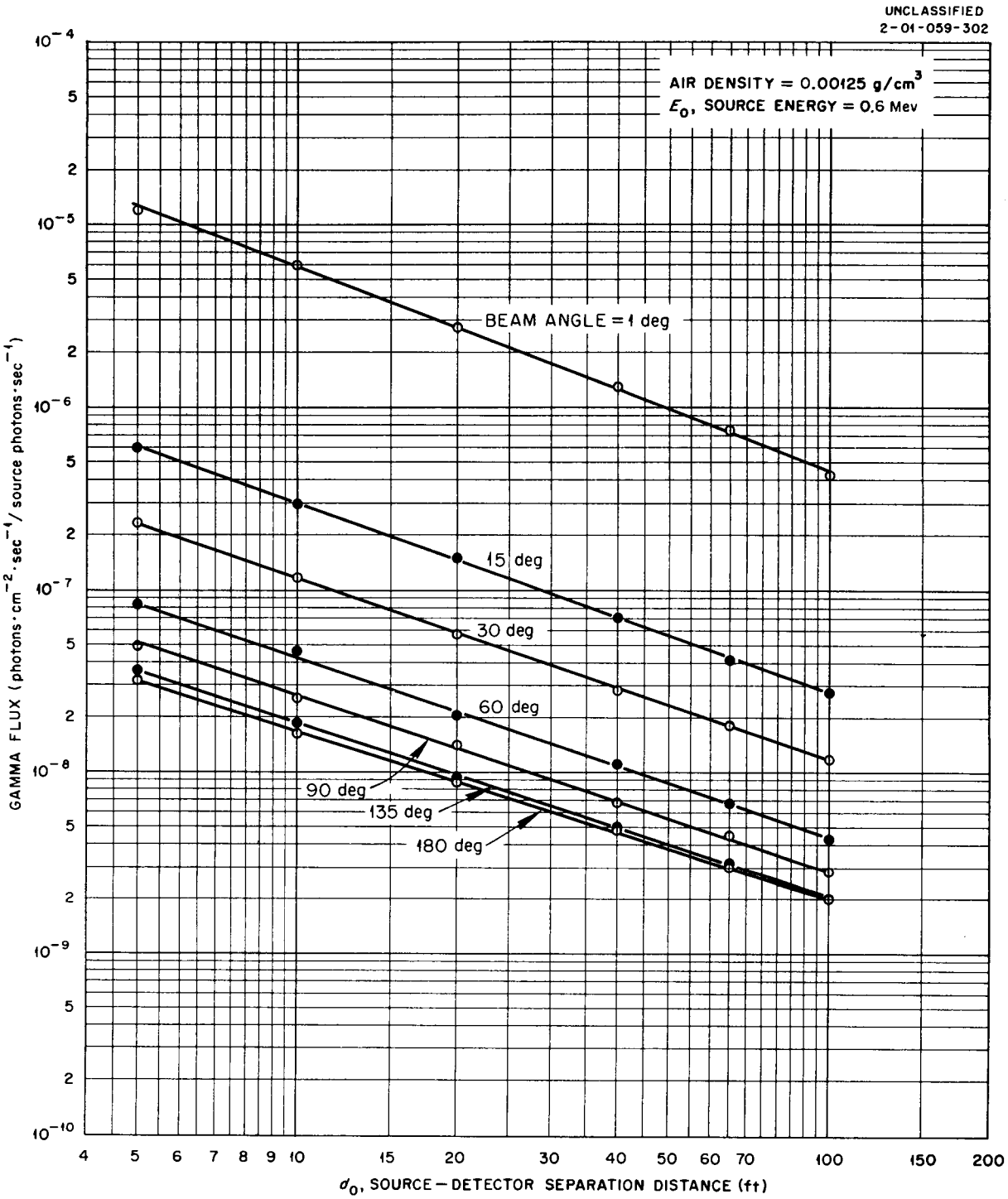

Fig. 10. Gamma-Ray Flux in Air as a Function of the Source-Detector Separation Distance: E_o = 0.6 Mev.

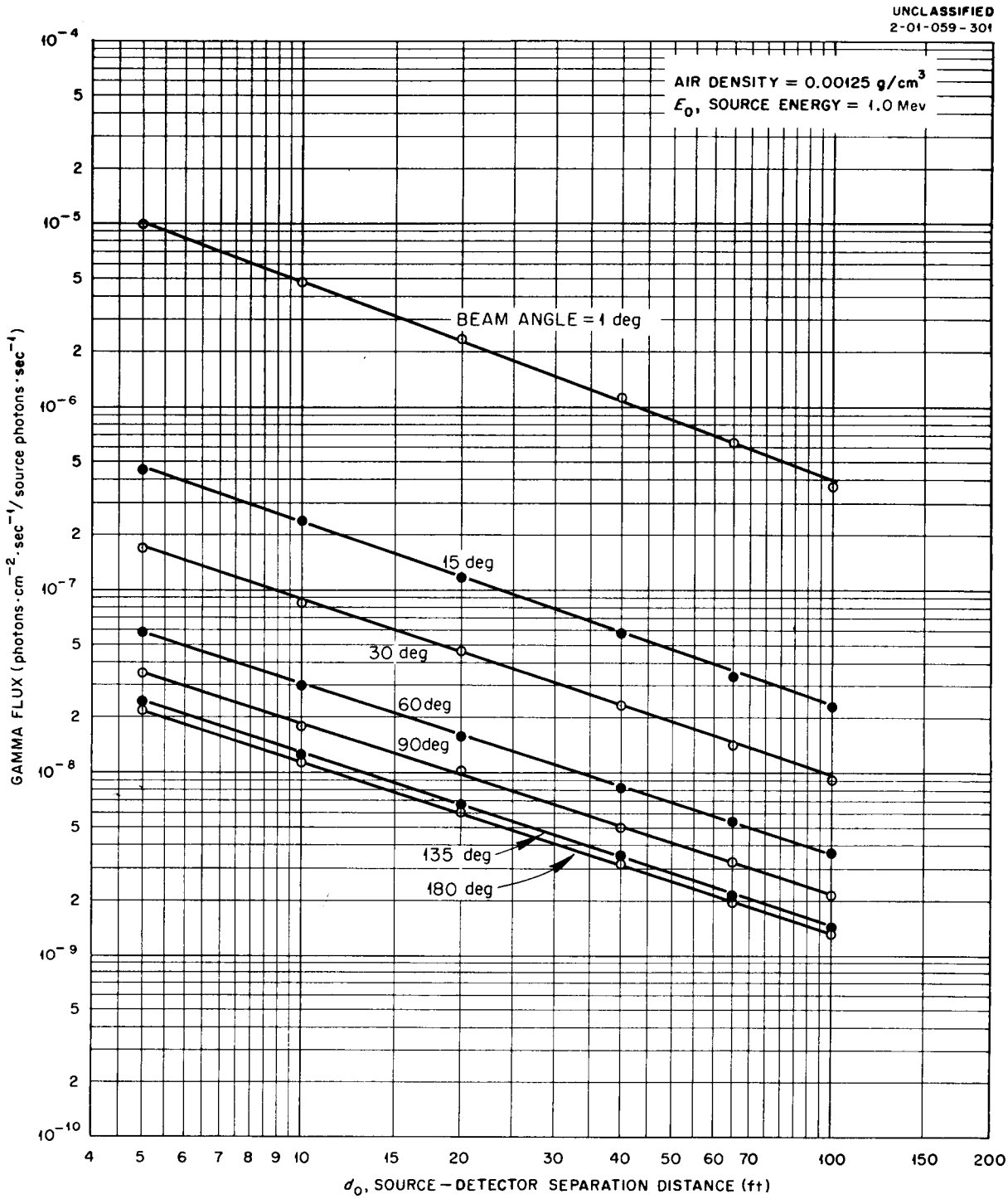

Fig. 11. Gamma-Ray Flux in Air as a Function of the Source-Detector Separation Distance: E_o = 1.0 Mev.

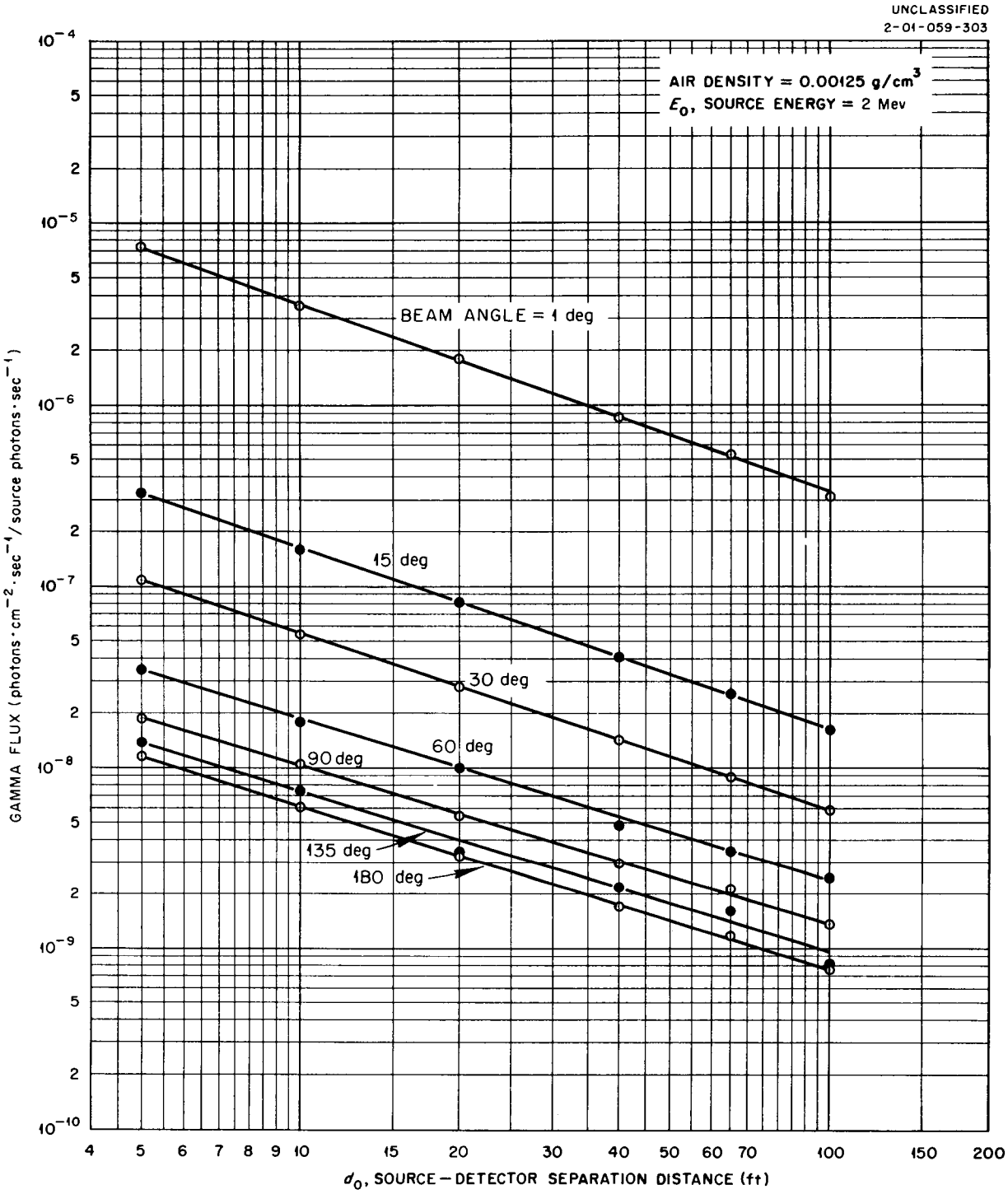

Fig. 12. Gamma-Ray Flux in Air as a Function of the Source-Detector Separation Distance: E_o = 2.0 Mev.

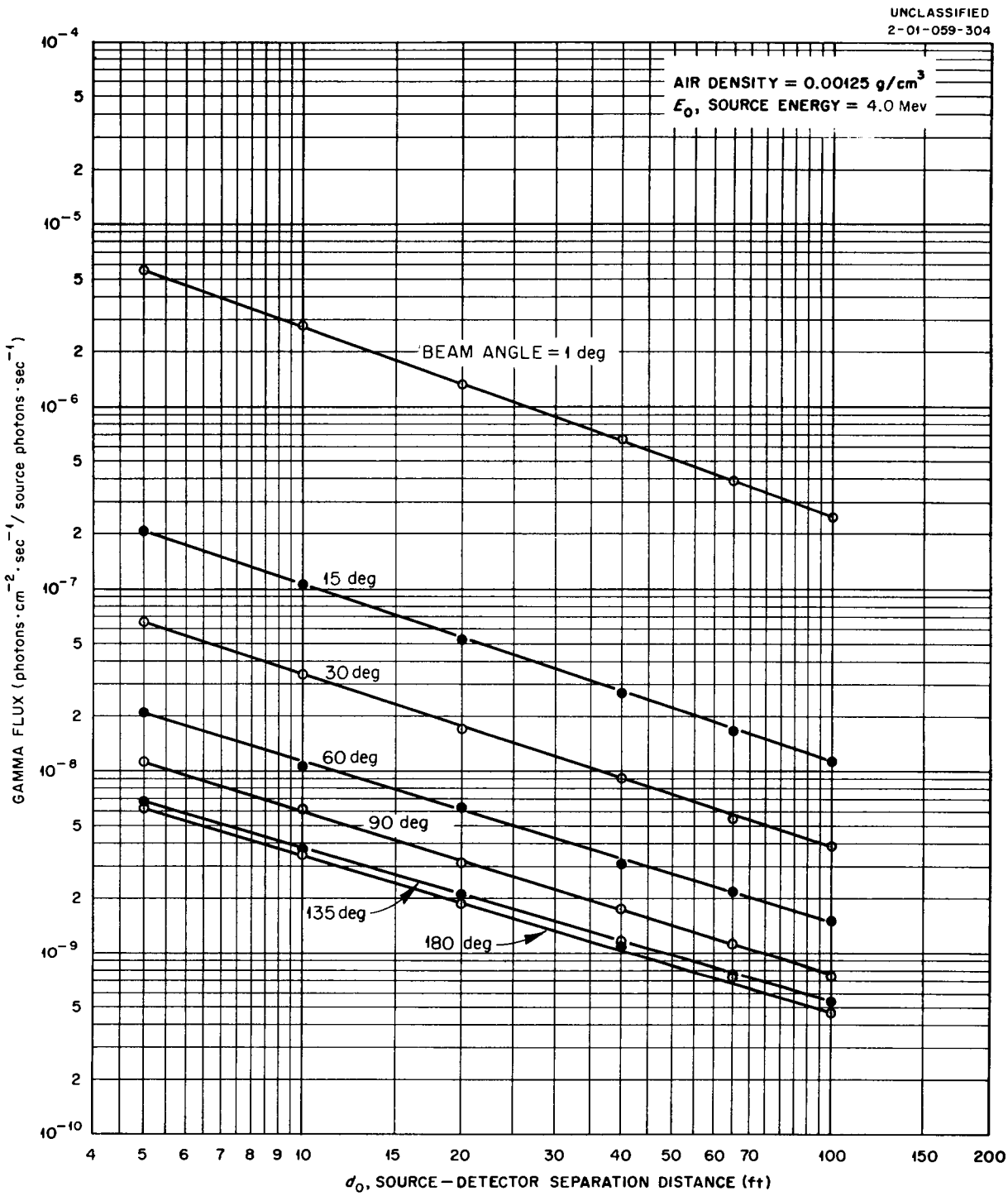

Fig. 13. Gamma-Ray Flux in Air as a Function of the Source-Detector Separation Distance: E_o = 4.0 Mev.

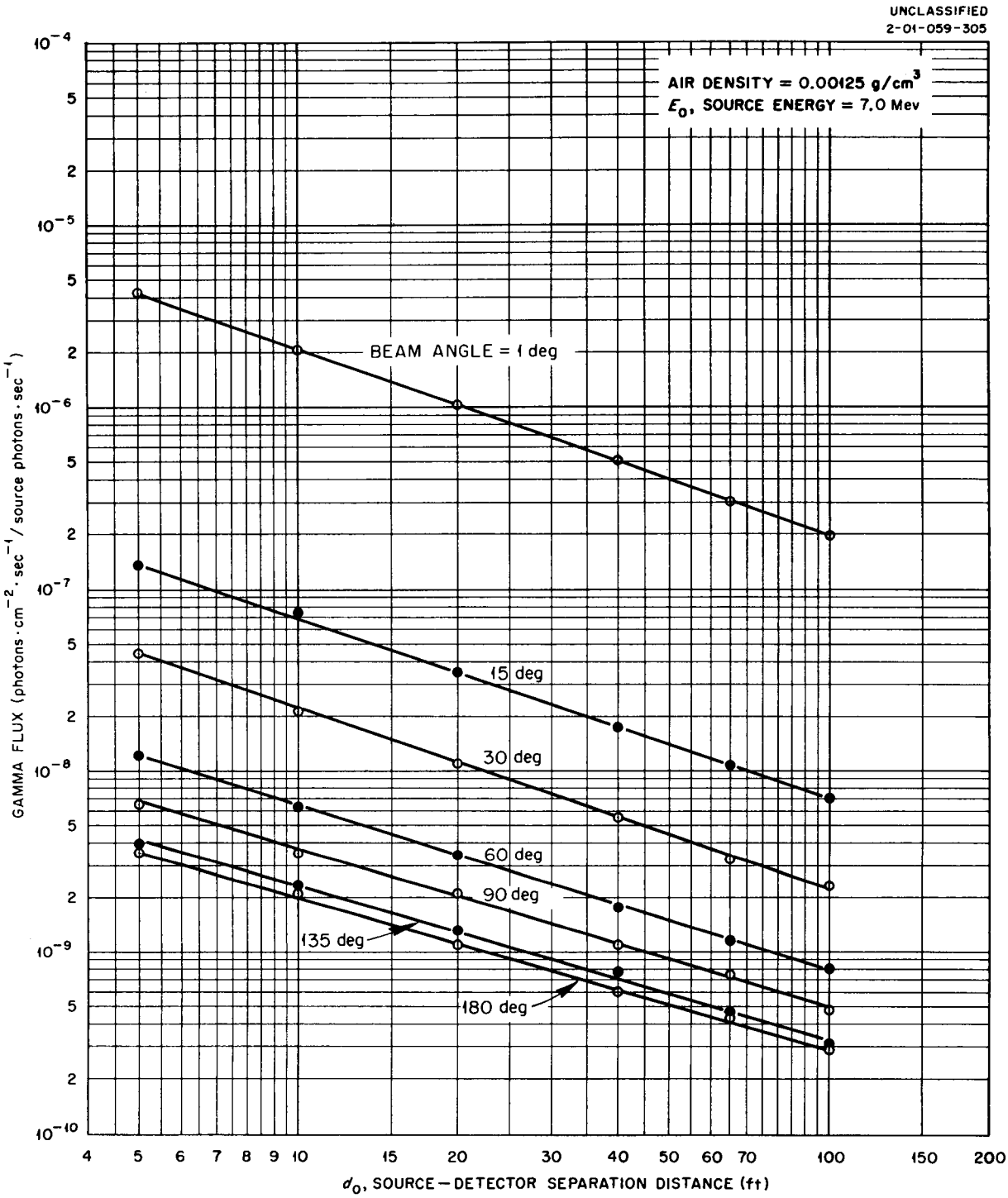

Fig. 14. Gamma-Ray Flux in Air as a Function of the Source-Detector Separation Distance: E_o = 7.0 Mev.

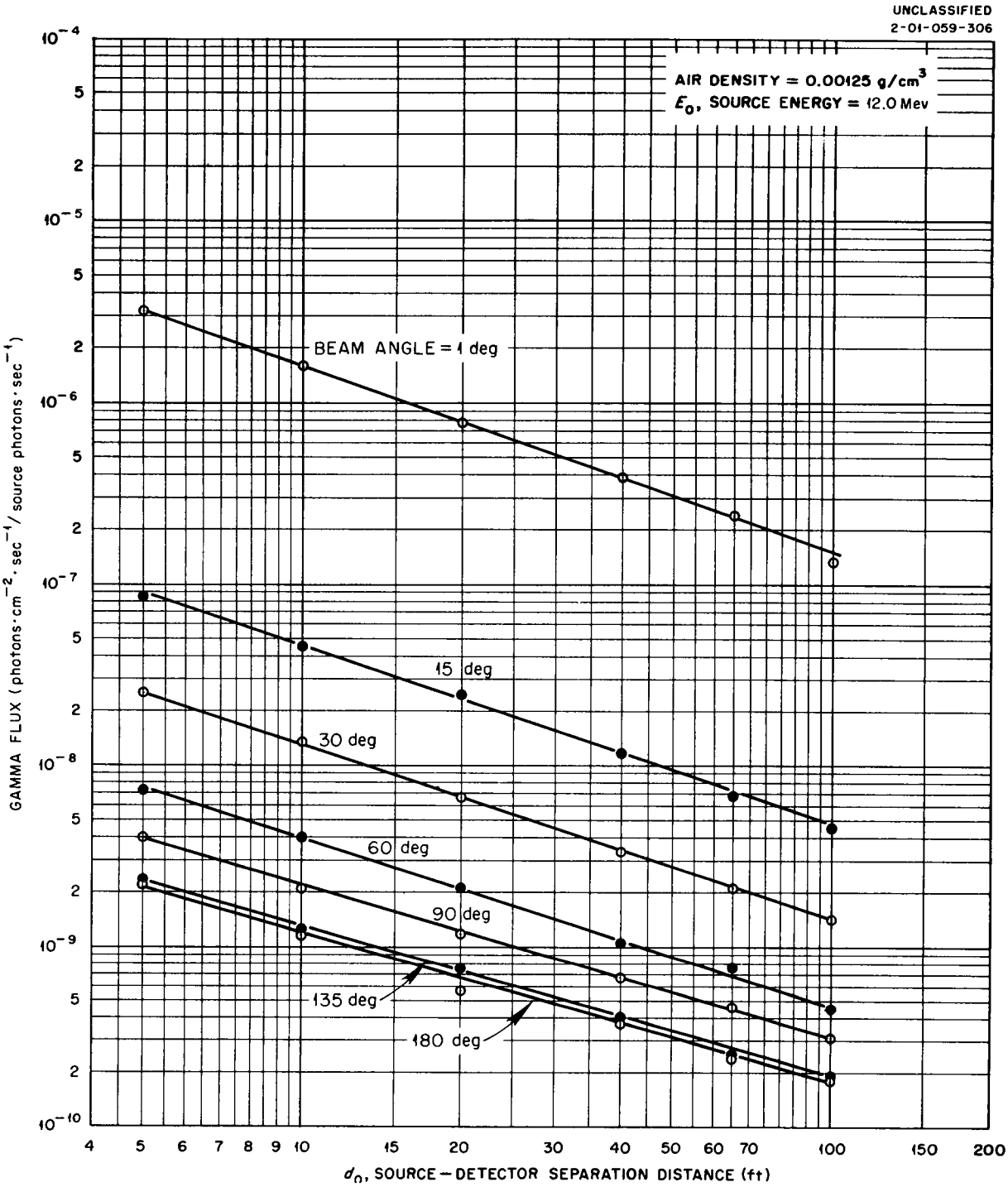

Fig. 15. Gamma-Ray Flux in Air as a Function of the Source-Detector Separation Distance: E_o = 12.0 Mev.

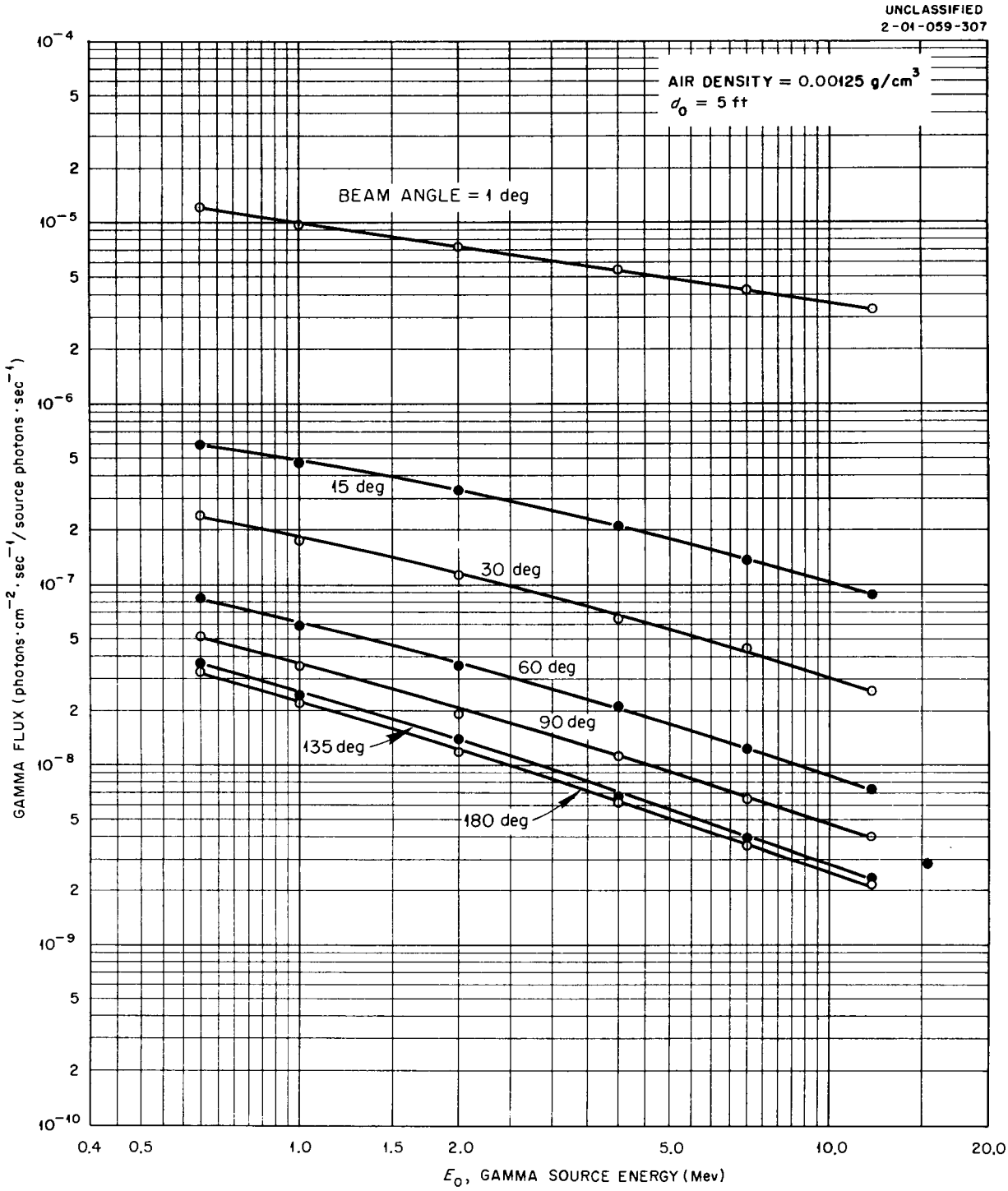

Fig. 16. Gamma-Ray Flux in Air as a Function of the Source Energy: d_o = 5 ft.

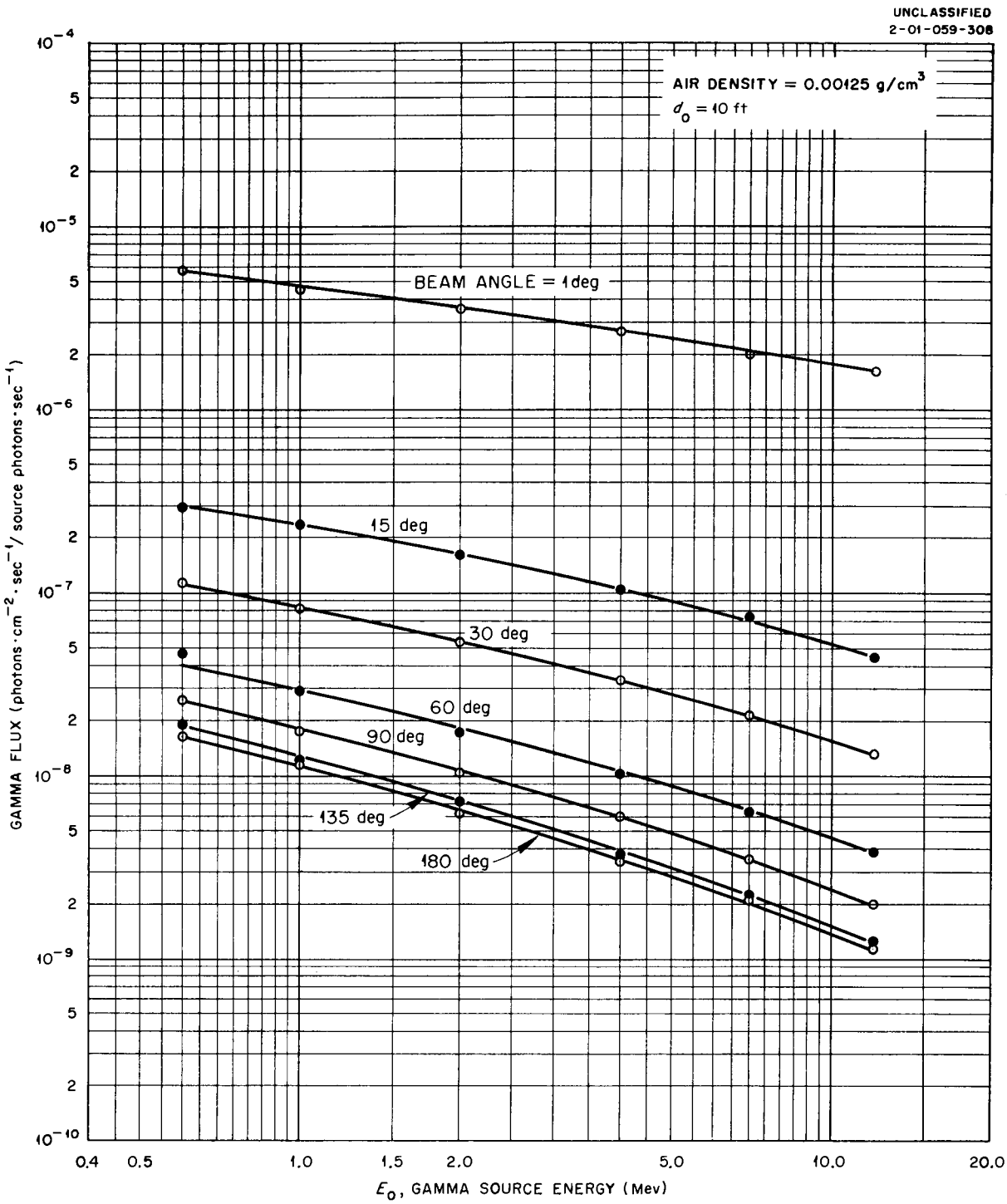

Fig. 17. Gamma-Ray Flux in Air as a Function of the Source Energy: d_o = 10 ft.

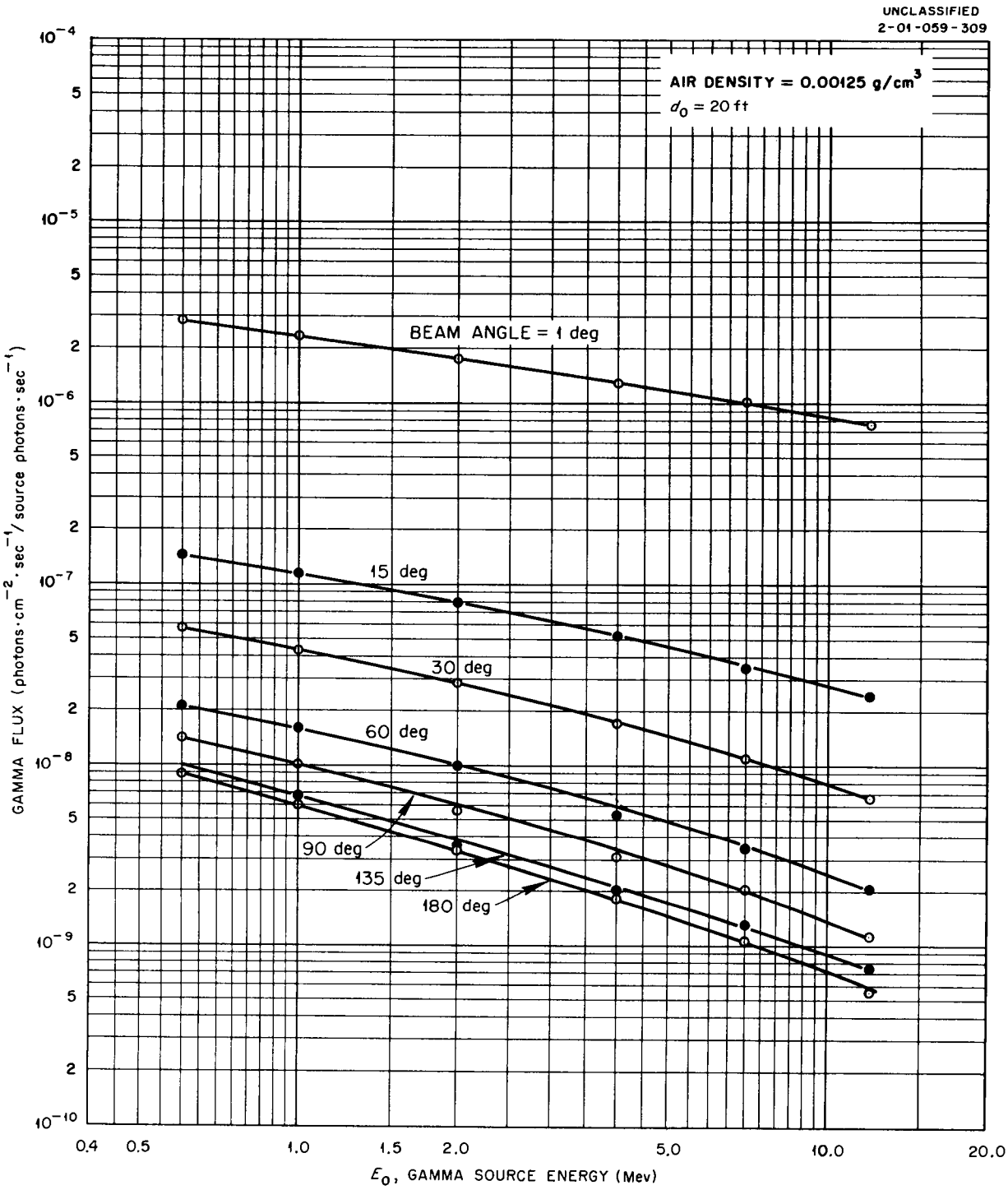

Fig. 18. Gamma-Ray Flux in Air as a Function of the Source Energy: d_o = 20 ft.

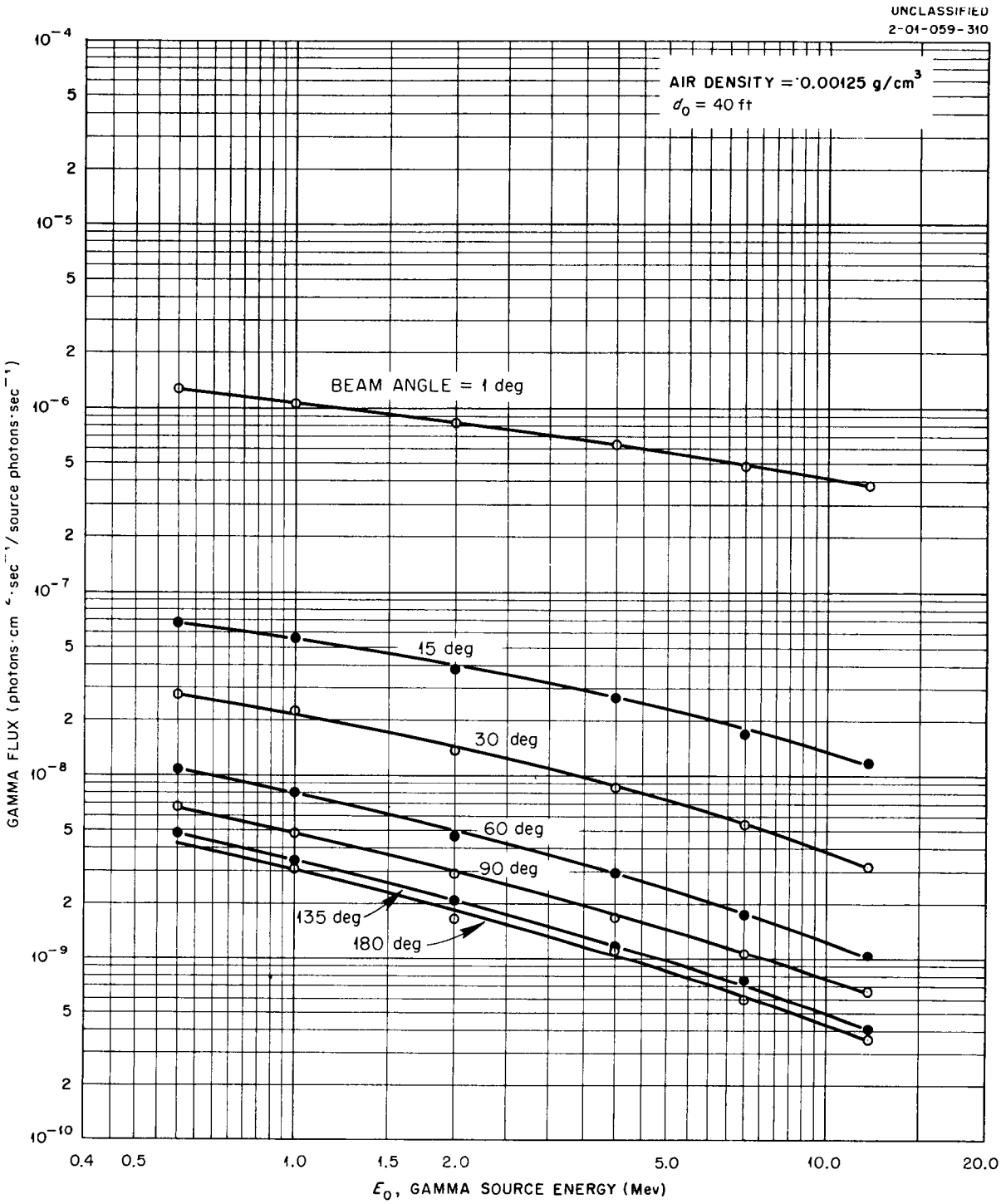

Fig. 19. Gamma-Ray Flux in Air as a Function of the Source Energy: d_o = 40 ft.

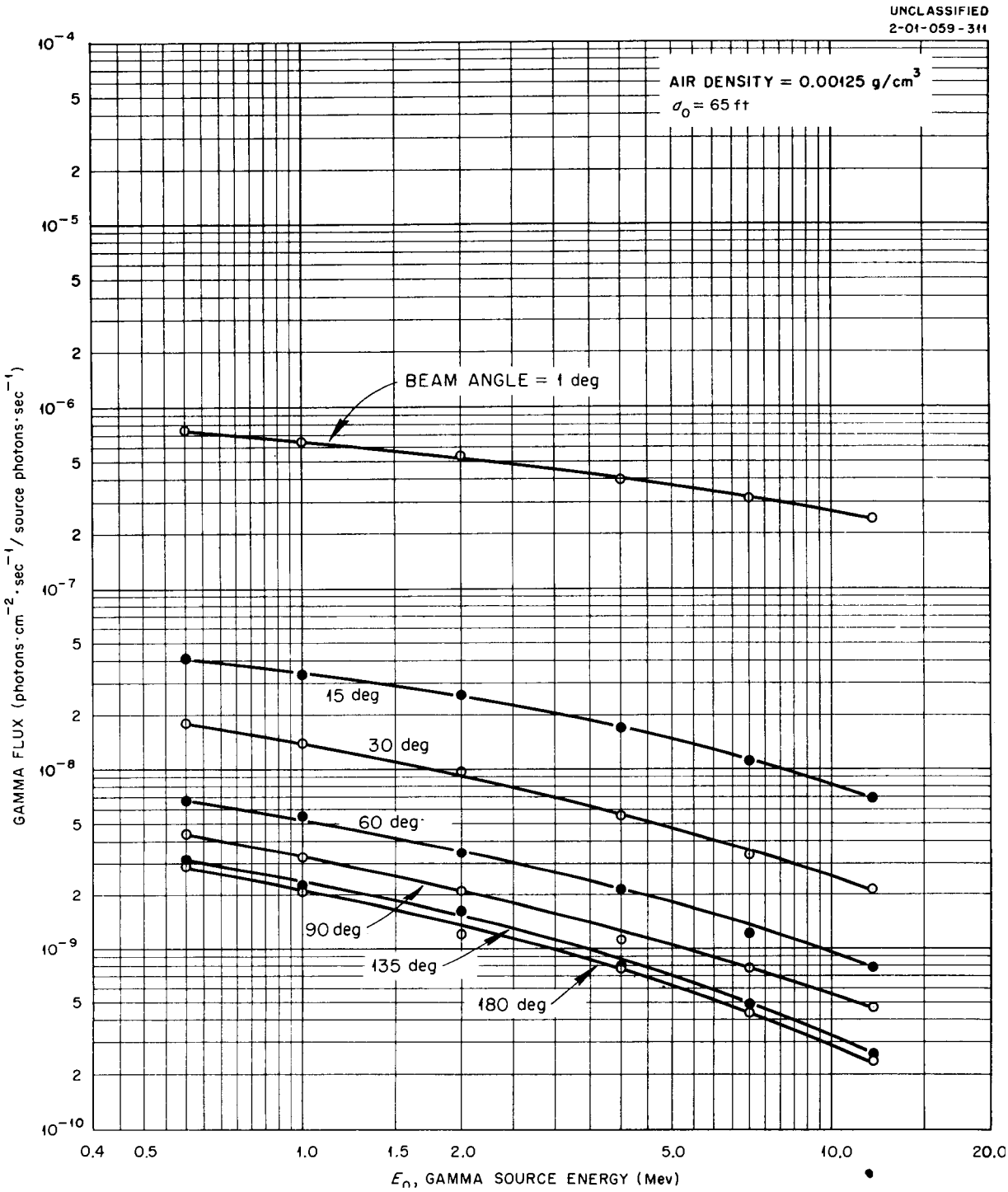

Fig. 20. Gamma-Ray Flux in Air as a Function of the Source Energy: d_o = 65 ft.

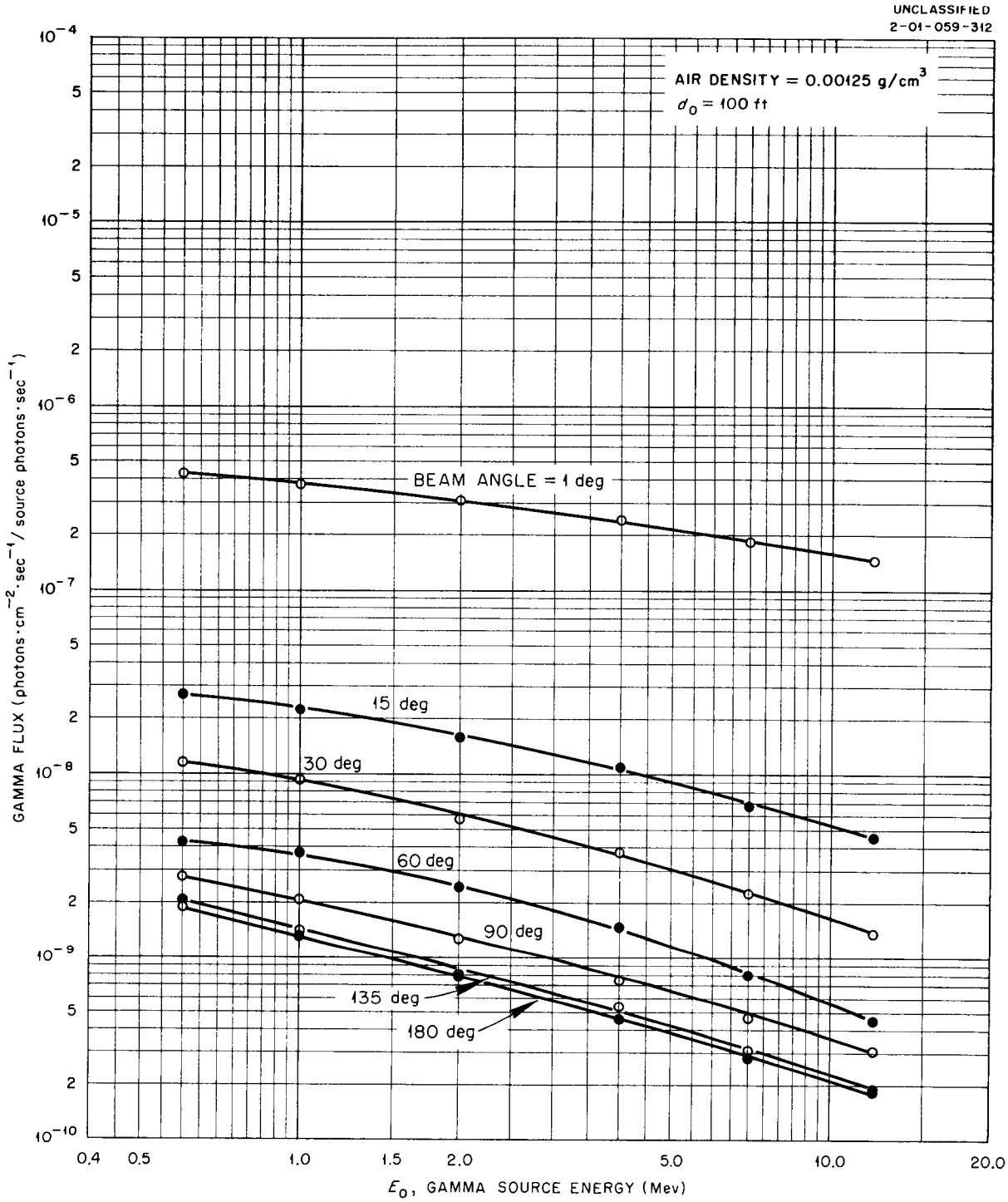

Fig. 21. Gamma-Ray Flux in Air as a Function of the Source Energy: d_o = 100 ft.

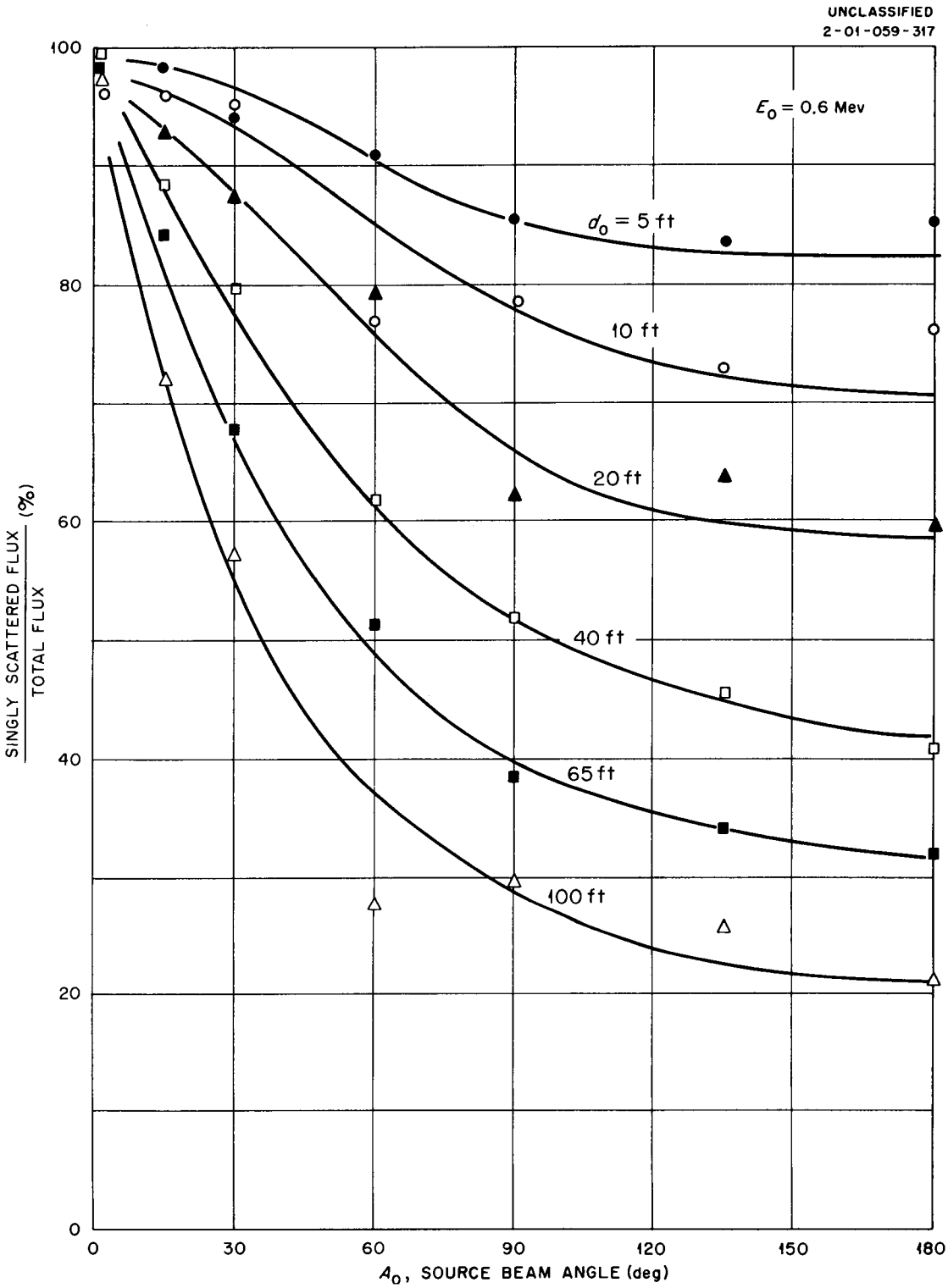

Fig. 22. Ratio of Singly Scattered Gamma-Ray Flux to the Total Flux as a Function of the Angle of Emission of the Source Beam: E_o = 0.6 Mev.

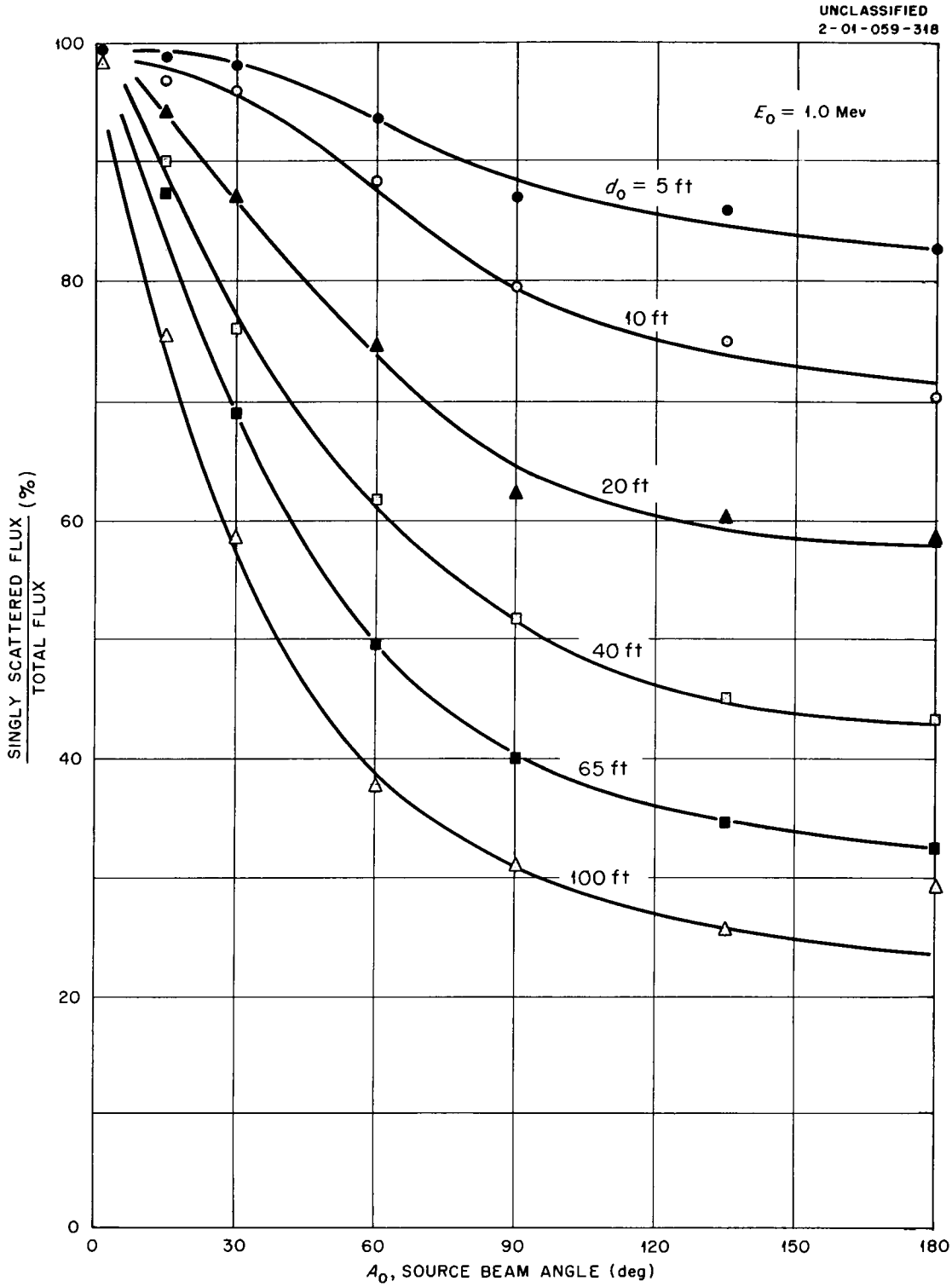

Fig. 23. Ratio of Singly Scattered Gamma-Ray Flux to the Total Flux as a Function of the Angle of Emission of the Source Beam: E_o = 1.0 Mev.

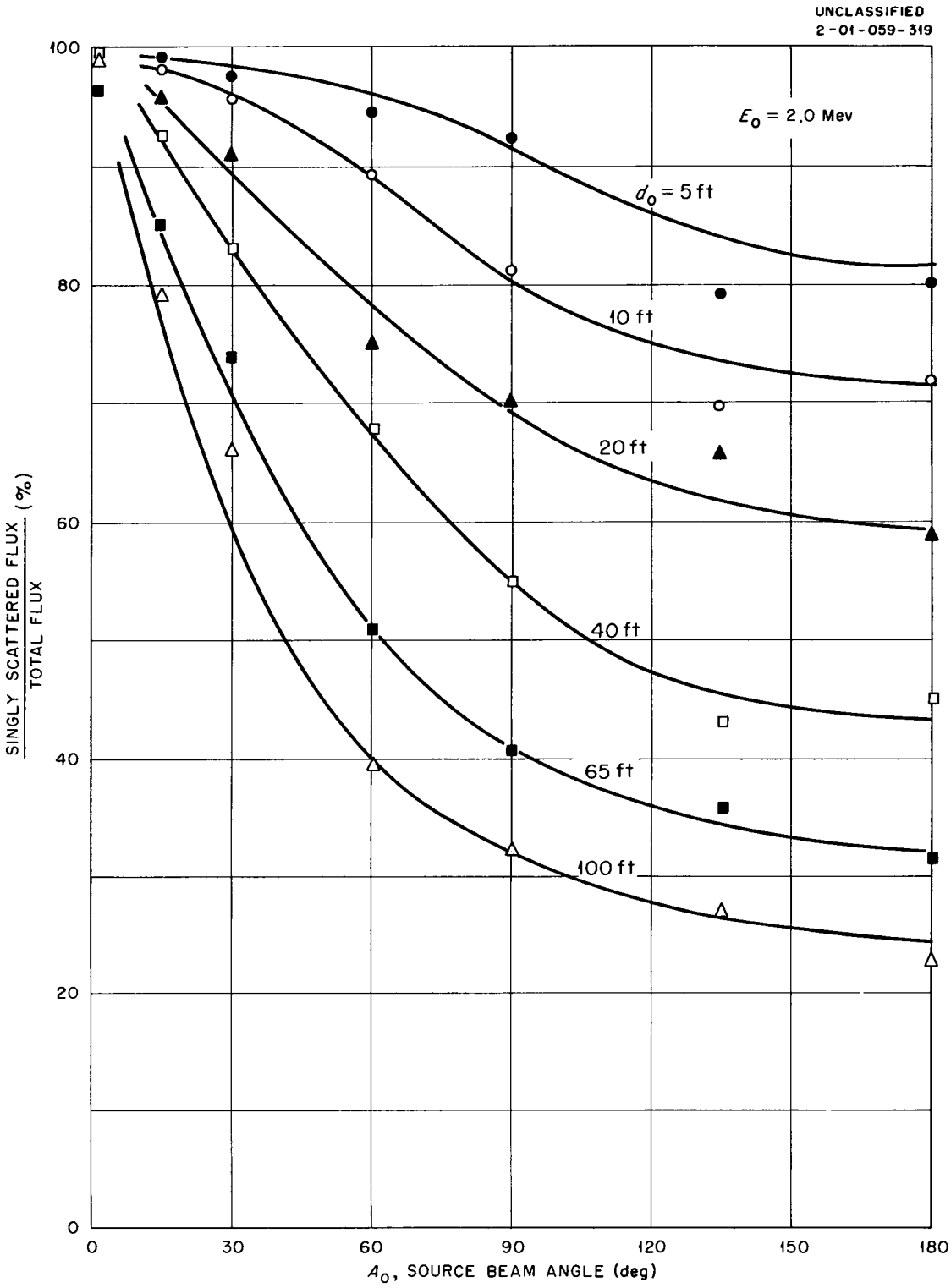

Fig. 24. Ratio of Singly Scattered Gamma-Ray Flux to the Total Flux as a Function of of the Angle of Emission of the Source Beam: E_o = 2.0 Mev.

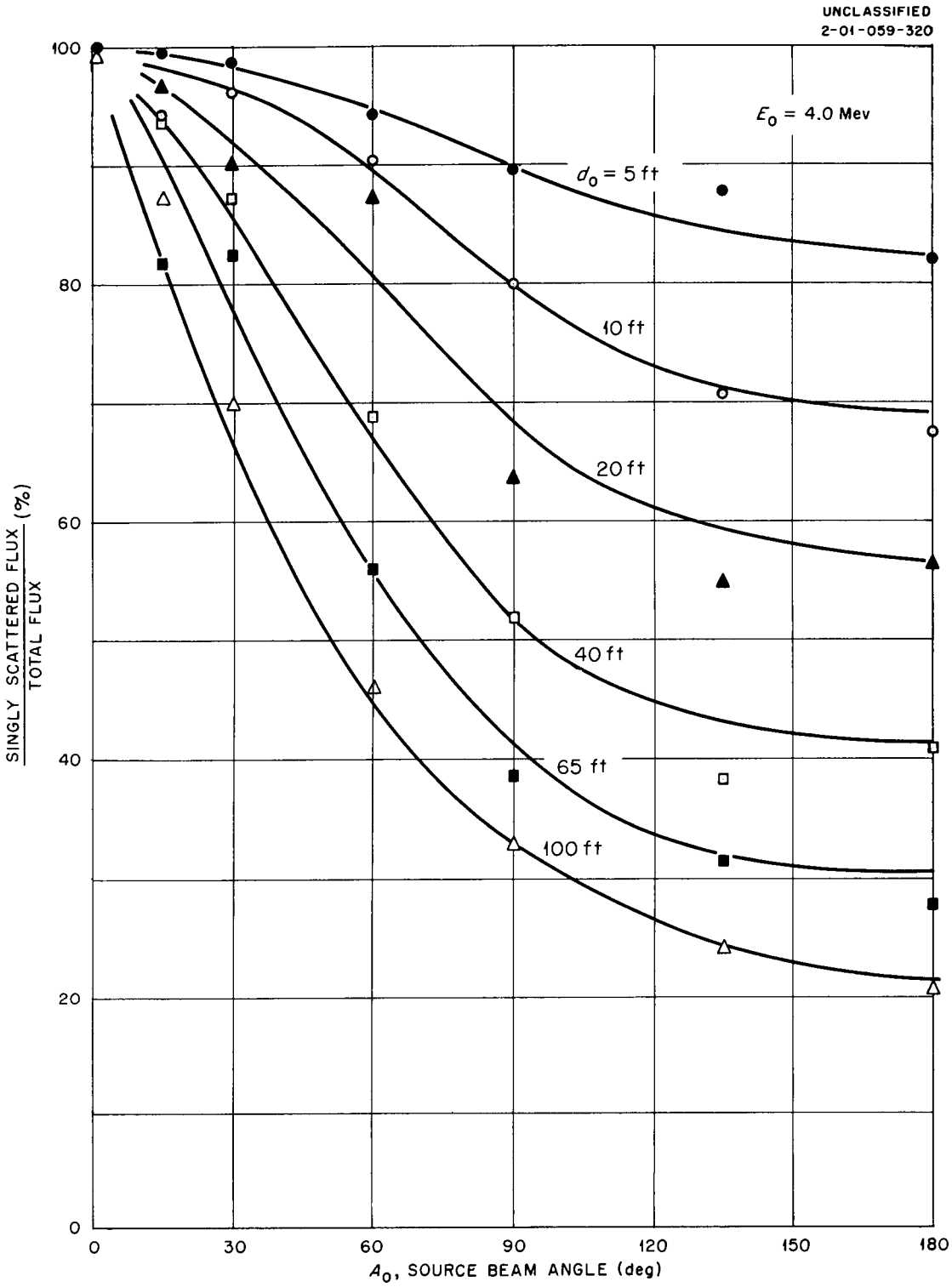

Fig. 25. Ratio of Singly Scattered Gamma-Ray Flux to the Total Flux as a Function of the Angle of Emission of the Source Beam: E_o = 4.0 Mev.

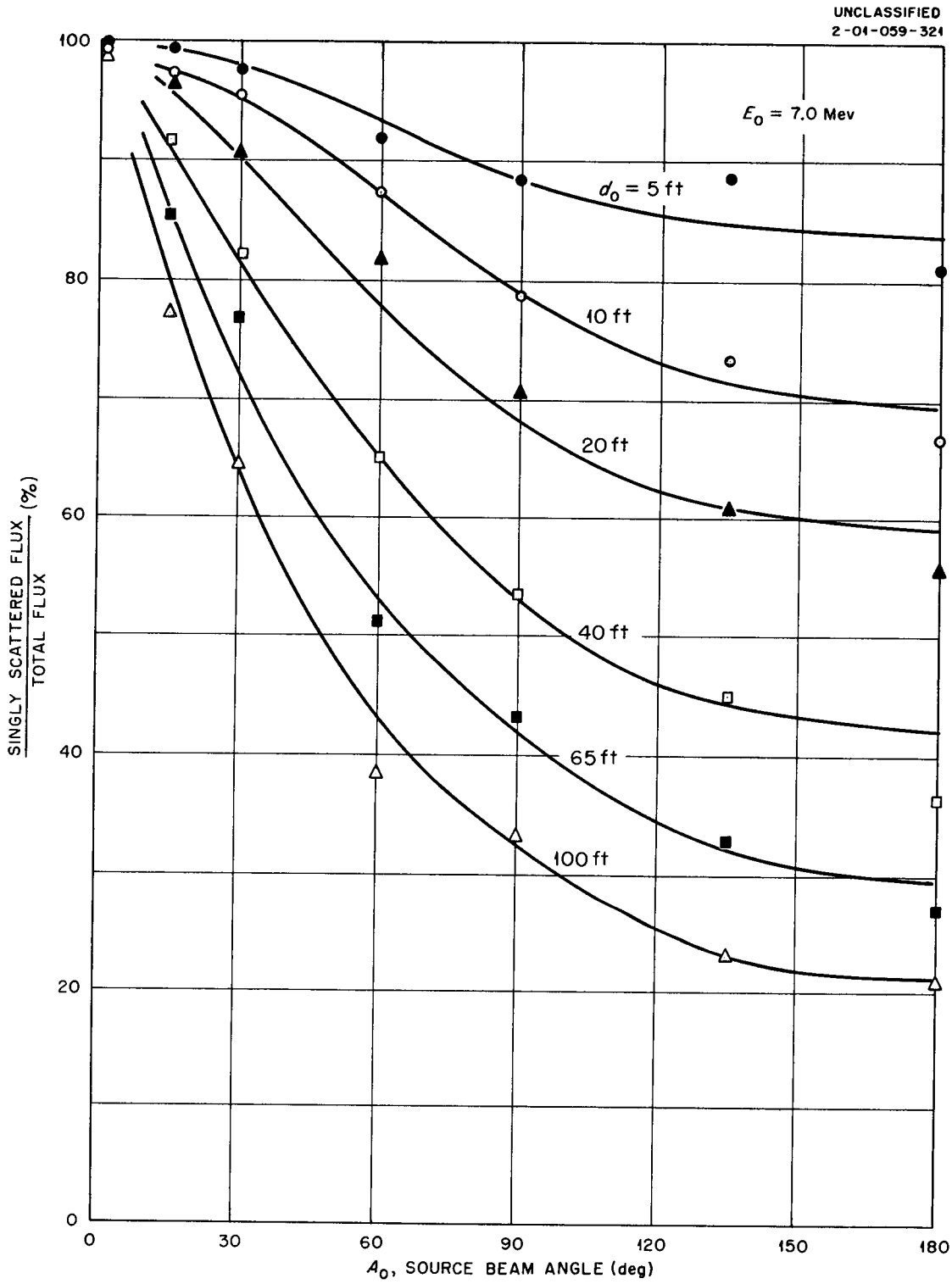

Fig. 26. Ratio of Singly Scattered Gamma-Ray Flux to the Total Flux as a Function of the Angle of Emission of the Source Beam: E_o = 7.0 Mev.

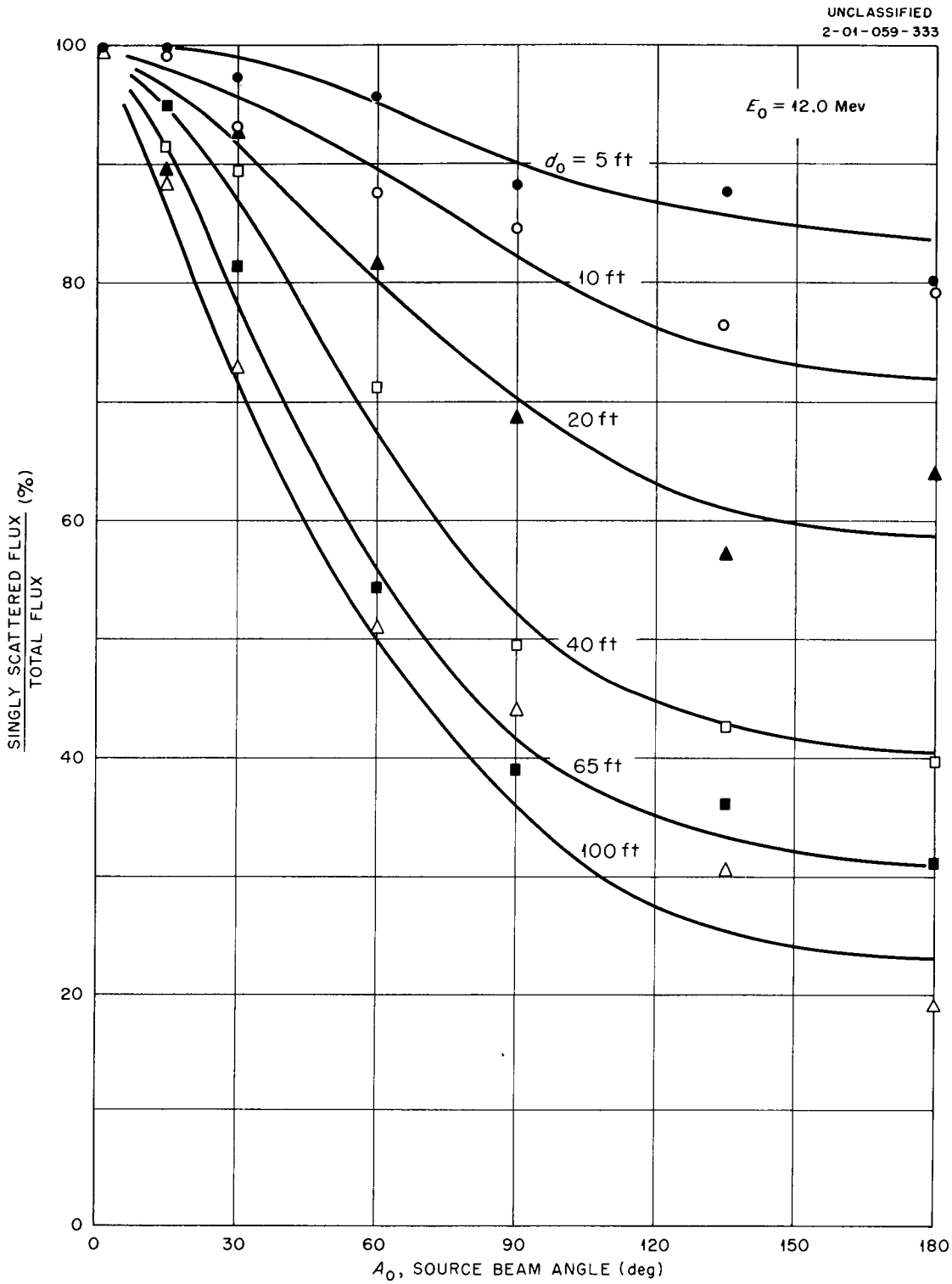

Fig. 27. Ratio of Singly Scattered Gamma-Ray Flux to the Total Flux as a Function of the Angle of Emission of the Source Beam: E_o = 12.0 Mev.

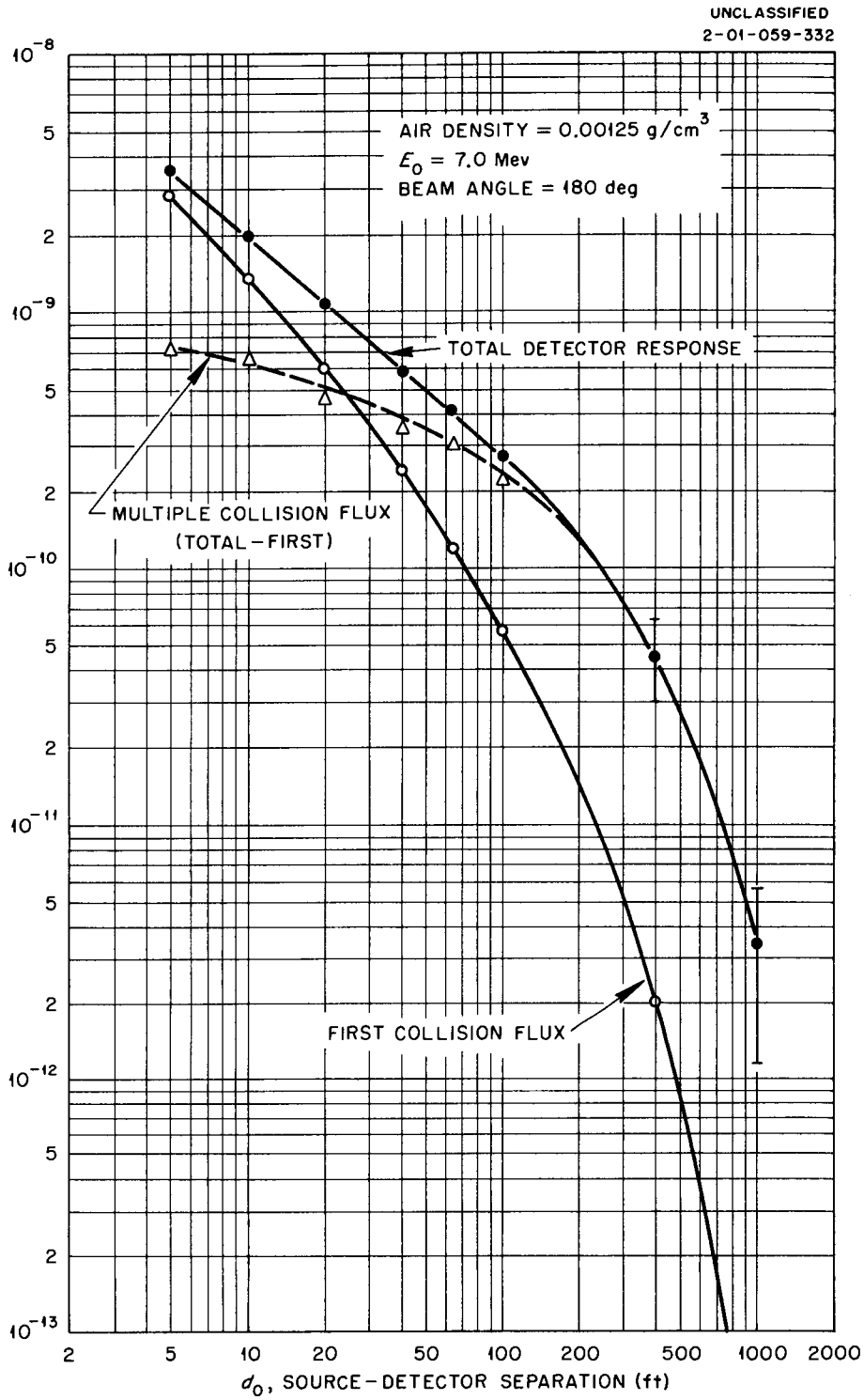

Fig. 28. Comparison of First-Collision, Multiple-Collision and Total Gamma-Ray Fluxes in Air as a Function of the Source-Detector Separation Distance: E_o = 7.0 Mev, A_o = 180 deg.

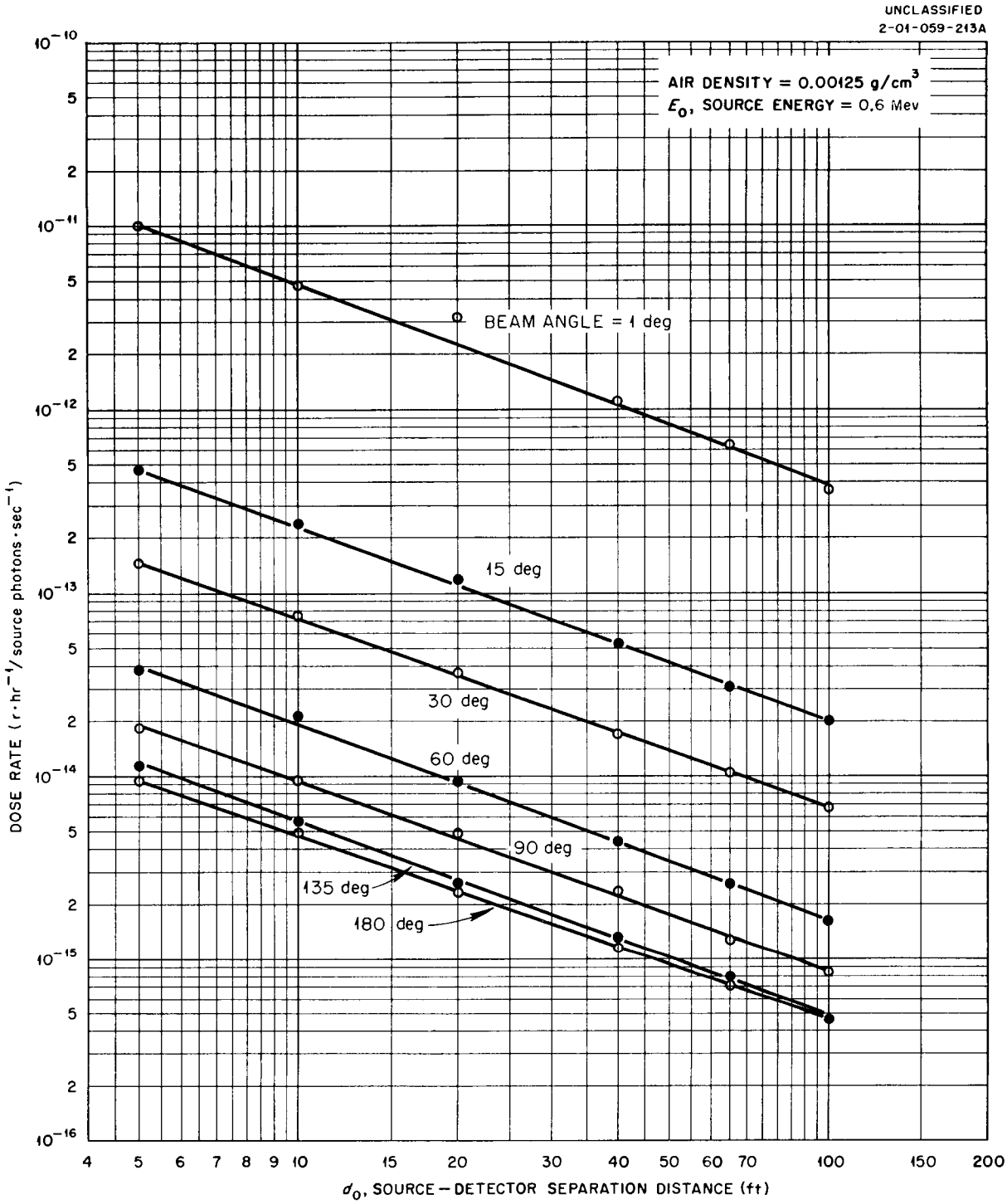

Fig. 29. Gamma-Ray Tissue Dose Rates in Air as a Function of the Source-Detector Separation Distance: E_o = 0.6 Mev.

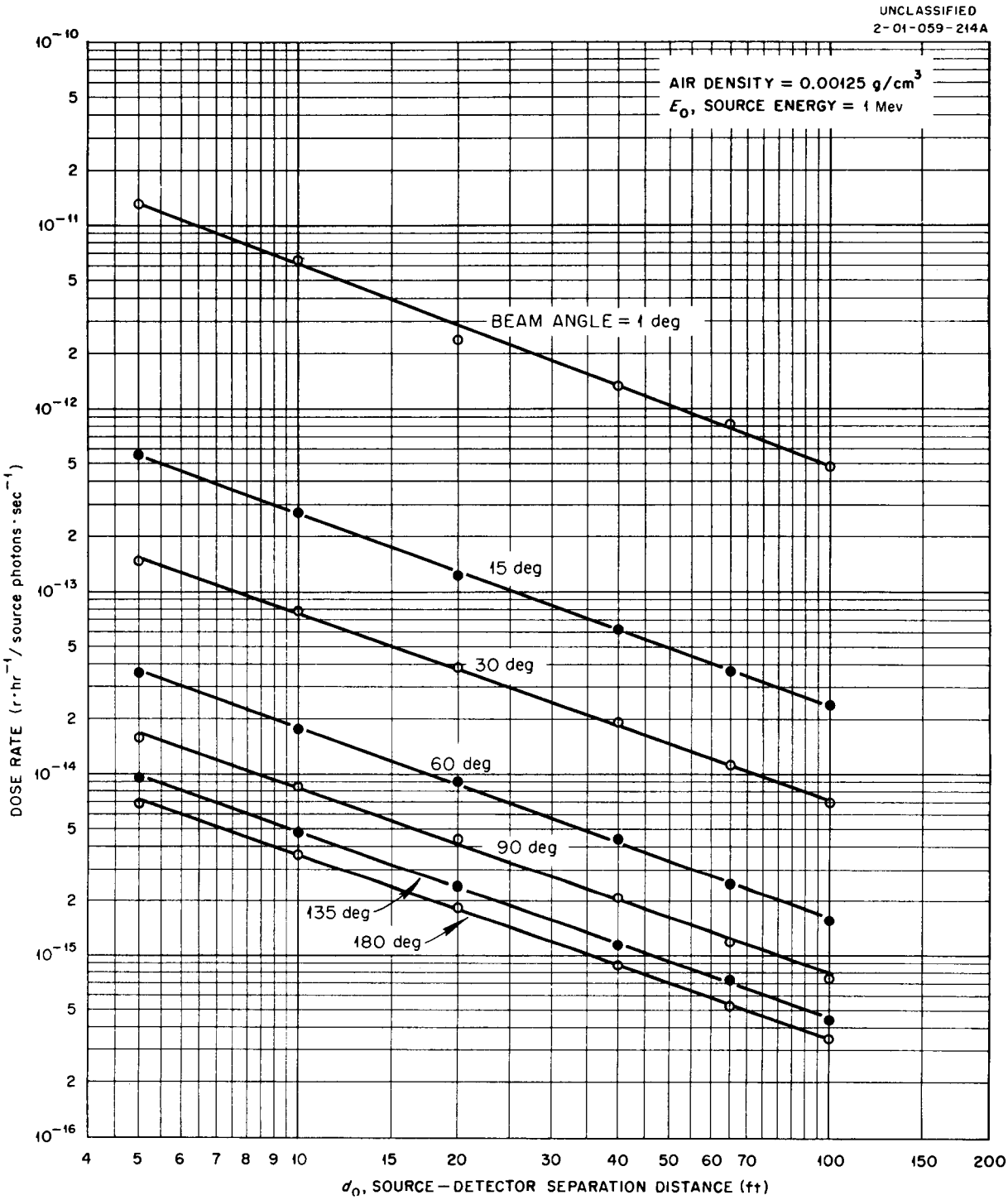

Fig. 30. Gamma-Ray Tissue Dose Rates in Air as a Function of the Source-Detector Separation Distance: E_o = 1 Mev.

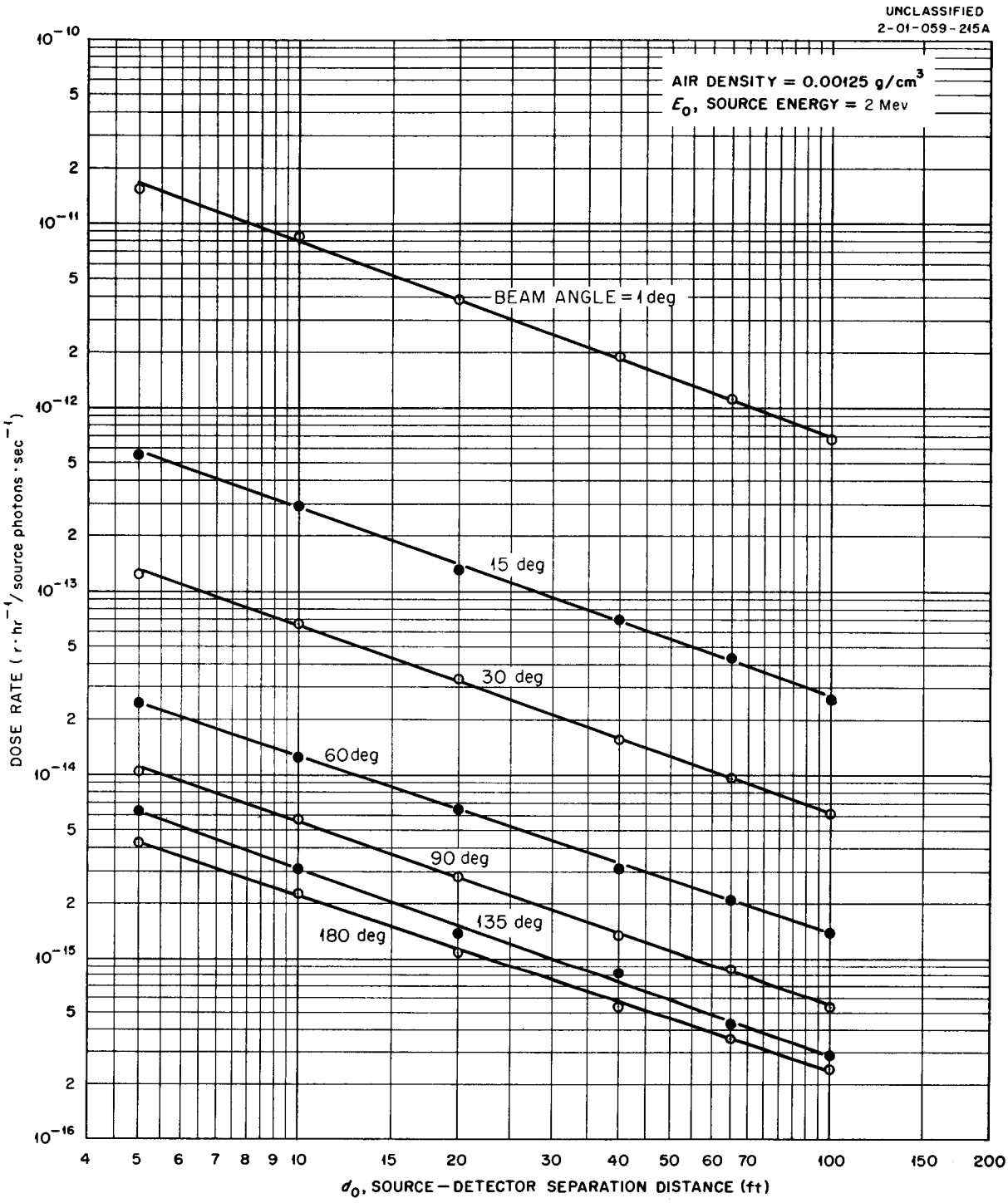

Fig. 31. Gamma-Ray Tissue Dose Rates in Air as a Function of the Source-Detector Separation Distance: E_o = 2 Mev.

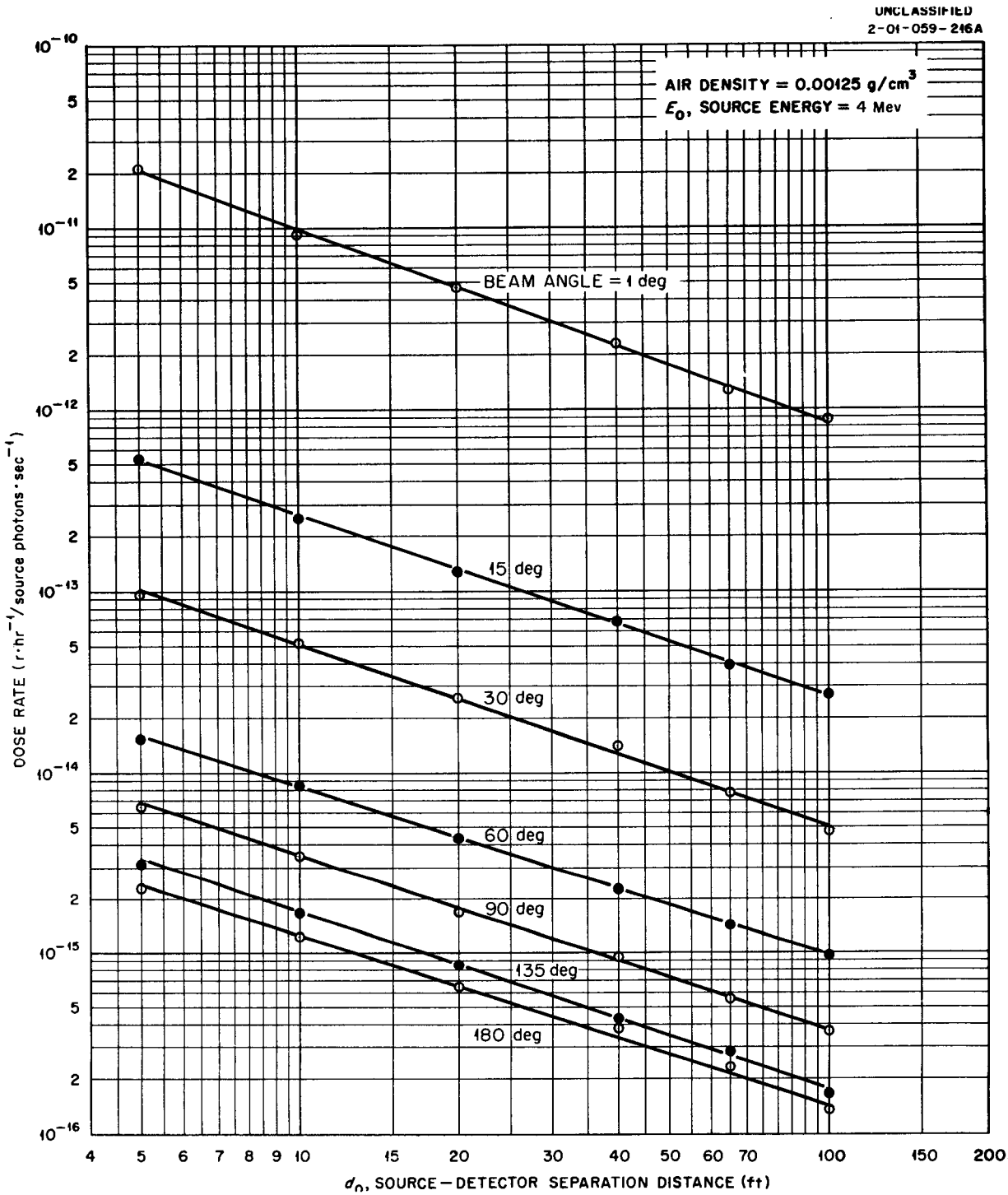

Fig. 32. Gamma-Ray Tissue Dose Rates in Air as a Function of the Source-Detector Separation Distance: E_o = 4 Mev.

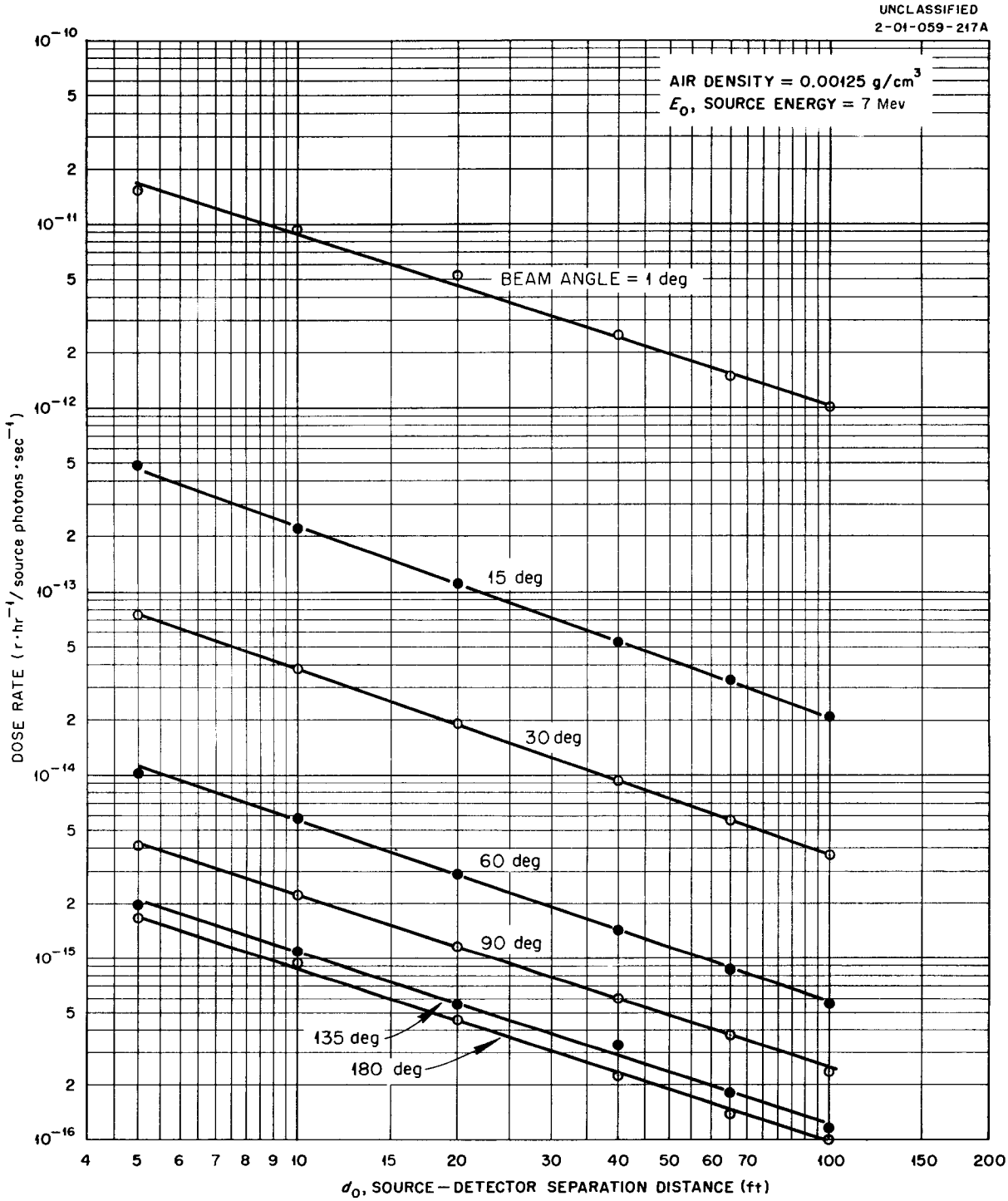

Fig. 33. Gamma-Ray Tissue Dose Rates in Air as a Function of the Source-Detector Separation Distance: E_o = 7 Mev.

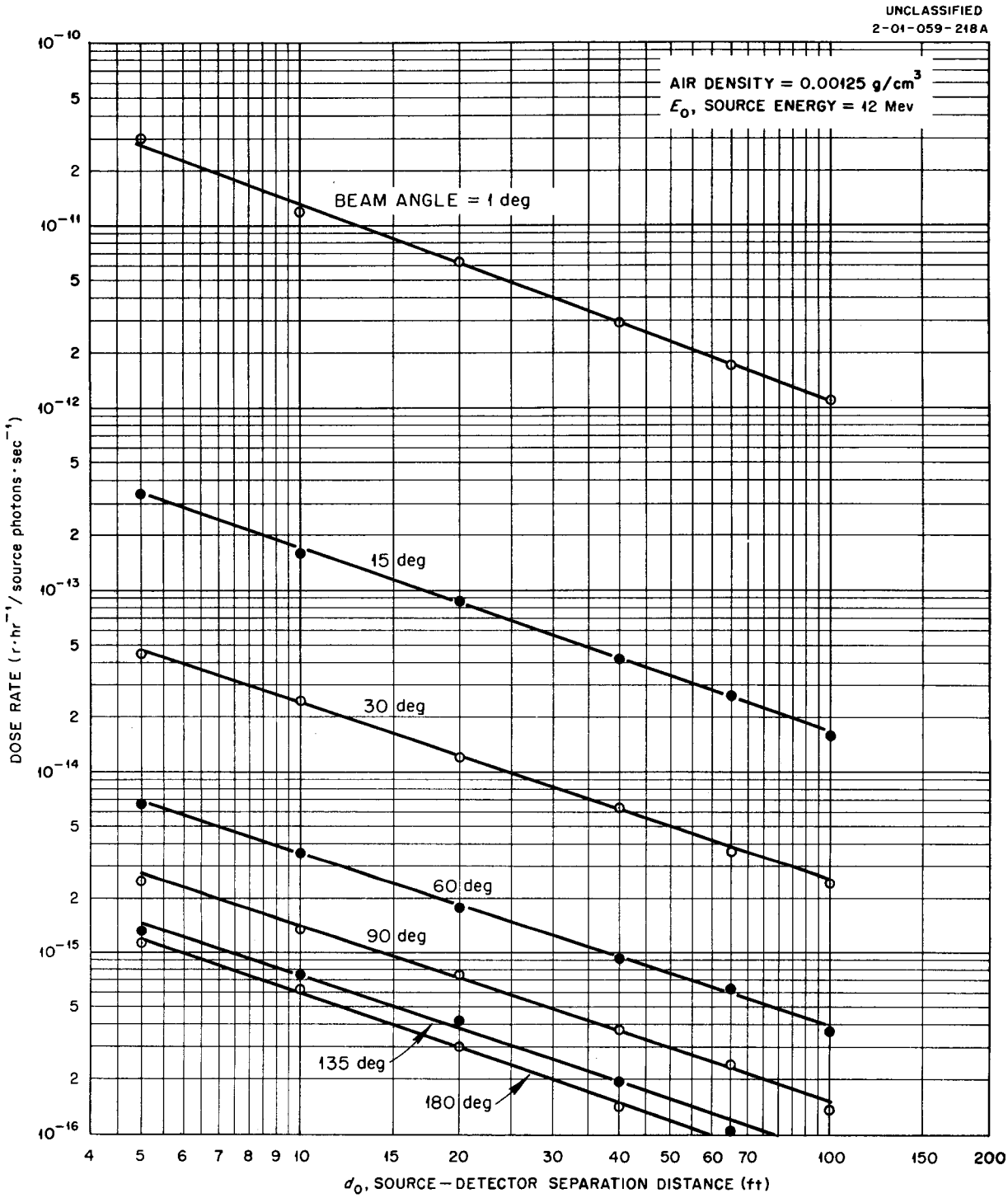

Fig. 34. Gamma-Ray Tissue Dose Rates in Air as a Function of the Source-Detector Separation Distance: E_o = 12 Mev.

Appendix A

LIST OF TABLES

Table No.	Title	Page No.
1	Numerical Values of the Source Parameters Which Were Used in the Computation	2
2	Polar and Azimuthal Angle Intervals at the Detector	2
3	Computed Values of Σ_t, σ_t/σ_c, and σ_c	9
4	Dose Rate Conversion Factors, T_e, for the Energy Intervals (E_e, E_{e+1}) Corresponding to Each Source Energy, E_o	21
5	First-Collision Contribution to the Flux at the Detector Resulting from a Point Monodirectional Source of Photons at a Beam Angle of 180 deg	35
6	First-Collision Contribution to the Flux at the Detector Resulting from a Point Monodirectional Source of Photons as a Beam Angle of 1 deg	35

Appendix B

LIST OF FIGURES

Fig. No.	Description	Page No.
1	Geometrical Relationship of Source and Detector	3
2	The Spacial Grid System at the Detector	3
3	Total Cross Section, Σ_t, Compton Cross Section, σ_c, and the Ratio σ_t/σ_c for Air as a Function of Energy	10
4	Tissue Gamma-Ray Dose Rate per Unit Photon Flux as a Function of Energy (Taken from TID-7004)	20
5	Schematic Diagram of the von Neumann Method of Selecting a Random Variable x from the Probability Density Function $f(x) = e^{-x}$ where $0 \leq x < \infty$	26
6	Schematic Diagram of the Method of Selecting Direction Cosines from the Isotropic Distribution	31
7	Solutions of the One-Velocity Boltzmann Equation for an Isotropic Point Source of Photons in an Infinite Medium of Air	33
8	Comparison of Some of the Results of 18 Different Calculations of Case 213: Photon Current Through Various Azimuthal Angle Intervals	36
9	Comparison of Some of the Results of 18 Different Calculations of Case 213: Photon Current Through a Solid Angle Interval and Total Detector Response	37
10	Gamma-Ray Flux at a Point Detector as a Function of the Distance Between the Detector and a Point Source Emitting a Monodirectional Beam of 0.6-Mev Gamma Rays at Various Angles: Air Medium	40
11	Same as Fig. 10 for E_o = 1.0 Mev	41
12	" 2.0 Mev	42
13	" 4.0 Mev	43
14	" 7.0 Mev	44
15	" 12.0 Mev	45

Fig. No.	Description	Page No.
16	Gamma-Ray Flux at a Point Detector as a Function of the Energy of Monoenergetic, Monodirectional Gamma Rays Emitted at Various Angles from a Point Source 5 ft from the Detector: Air Medium	46
17	Same as Fig. 16 for d_o = 10 ft	47
18	" 20 ft	48
19	" 40 ft	49
20	" 65 ft	50
21	" 100 ft	51
22	Ratio of Singly Scattered Gamma-Ray Flux to the Total Flux at a Point Detector as a Function of the Angle of Emission of a Monodirectional Beam of 0.6-Mev Gamma Rays from a Point Source Located at Various Distances (d_o) from the Detector: Air Medium	52
23	Same as Fig. 22 for E_o = 1.0 Mev	53
24	" 2.0 Mev	54
25	" 4.0 Mev	55
26	" 7.0 Mev	56
27	" 12.0 Mev	57
28	Comparison of First-Collision, Multiple-Collision and Total Gamma-Ray Fluxes at a Point Detector as a Function of the Distance Between the Detector and a Point Source Emitting a Beam of 7.0-Mev Gamma Rays at an Angle of 180 deg: Air Medium	58
29	Gamma-Ray Tissue Dose Rates at a Point Detector as a Function of the Distance Between the Detector and a Point Source Emitting a Monodirectional Beam of 0.6-Mev Gamma Rays at Various Angles: Air Medium	59
30	Same as Fig. 29 for E_o = 1 Mev	60
31	" 2 Mev	61
32	" 4 Mev	62
33	" 7 Mev	63
34	" 12 Mev	64

ORNL-2292
Volume 1
Physics and Mathematics*

INTERNAL DISTRIBUTION

1. C. E. Center
2. Biology Library
3. Health Physics Library
4-5. Central Research Library
6. Reactor Experimental Engineering Library
7-26. Laboratory Records Department
27. Laboratory Records, ORNL R.C.
28. A. M. Weinberg
29. L. B. Emlet (K-25)
30. J. P. Murray (Y-12)
31. J. A. Swartout
32. E. H. Taylor
33. E. D. Shipley
34. A. H. Snell
35. E. P. Blizard
36. M. L. Nelson
37. W. H. Jordan
38. G. E. Boyd
39. R. A. Charpie
40. S. C. Lind
41. F. L. Culler
42. A. Hollaender
43. J. H. Frye, Jr.
44. M. T. Kelley
45. J. L. Fowler
46. R. S. Livingston
47. K. Z. Morgan
48. T. A. Lincoln
49. A. S. Householder
50. C. P. Keim
51. C. A. Preskitt
52. C. E. Winters
53. D. S. Billington
54. H. E. Seagren
55. D. Phillips
56. A. J. Miller
57. M. J. Skinner
58. R. R. Dickison
59. J. A. Harvey
60. A. Simon
61. F. C. Maienschein
62. C. E. Clifford
63. A. D. Callihan
64. R. R. Coveyou
65. W. Zobel
66. F. L. Keller
67. C. D. Zerby
68. D. K. Trubey
69. S. K. Penny
70. R. W. Peelle
71. E. G. Silver
72. G. deSaussure
73. V. R. Cain
74. L. B. Holland
75. L. Jung
76. G. T. Chapman
77. M. J. Muckenthaler
78. R. B. Murray
79. Francis Alsmiller
80. R. Aronson (consultant)
81. F. L. Friedman (consultant)
82. H. Goldstein (consultant)
83. H. Hurwitz, Jr. (consultant)
84. L. W. Nordheim (consultant)
85. R. R. Wilson (consultant)
86. ORNL - Y-12 Technical Library, Document Reference Section

EXTERNAL DISTRIBUTION

87. Argonne National Laboratory (B. I. Spinrad)
88. Consolidated Vultee Aircraft Corporation (N. M. Schaffer)
89-90. Convair - General Dynamics (1 copy each for C. E. Chapman, Dr. Donaldson)
91. Curtiss-Wright Corporation (K. L. Rooney)
92-97. General Electric Company (ANPD) (1 copy each for F. A. Aschenbrenner, J. MacDonald, W. E. Edwards, J. Carver, R. H. Clark, and L. S. Burns)

---

*Because Volumes 2-5 total approximately 1050 pages and will be of limited interest, they have not been sent to all recipients listed on the distribution of Volume 1. However, Volumes 2-5 will be made available upon request.

98-99. Lockheed Aircraft Corporation (1 copy each for J. C. Flack and F. N. Watson)
100. National Advisory Committee for Aeronautics, Cleveland (I. M. Karp)
101-103. The Martin Company (1 copy each for G. Rausa, C. R. Fink, and F. N. Greene)
104-109. Wright Air Development Center (1 copy each for H. C. Thacker, WCLJC; Capt. E. J. Zawalick, WCLJX; G. Blanch, WCRRM; Lt. V. Shields, WCLPU; L. A. Bowman, WCLJX; and L. L. Antes, WCRRX)
110-713. Given distributions as shown in TID-4500 (13th Ed., Rev.) under Physics and Mathematics category (75 copies - OTS)